Review

Thermal analysis of mammalian stratum corneum using differential scanning calorimetry for advancing skin research and drug delivery

Choon Fu Goh[a,] *, Jonathan Hadgraft[b], Majella E Lane[b,] *

[a]*Discipline of Pharmaceutical Technology, School of Pharmaceutical Sciences, Universiti Sains Malaysia, 11800 Minden, Penang, Malaysia*

[b]*Department of Pharmaceutics, UCL School of Pharmacy, 29-39 Brunswick Square, London WC1N 1AX, Kingdom*

*Corresponding author.

Choon Fu Goh. Discipline of Pharmaceutical Technology, School of Pharmaceutical Sciences, Universiti Sains Malaysia, 11800 Minden, Penang, Malaysia. Tel.: +604-6532074; fax: +604-6570017

Email address: choonfugoh@usm.my

Majella E Lane. Department of Pharmaceutics, UCL School of Pharmacy, 29-39 Brunswick Square, London WC1N 1AX, Kingdom. Tel.: 0207 7535821 (Ex: +442039872851)

Email address: m.lane@ucl.ac.uk

Abstract

For effective topical and transdermal drug delivery, it is necessary for most actives to penetrate and permeate through the stratum corneum (SC). Extensive investigation of the thermal behaviour of mammalian SC has been performed to understand the barrier function of the skin. However, little attention has been paid to the related experimental variables that may influence the results obtained from such studies. In this review, we provide a comprehensive overview of the thermal transitions of the SC of both porcine and human skin. More importantly, the selection and impact of the experimental and instrumental parameters used in thermal analysis of the SC are critically evaluated. New opportunities for the use of thermal analysis of mammalian SC in advancing skin research, particularly for elucidation of the actions of excipients employed in topical and transdermal formulations on the skin are also highlighted.

Keywords: Mammalian skin; stratum corneum; differential scanning calorimetry; skin lipids; keratin protein; excipients; skin permeation

Abbreviations:

CA-SCS: Sodium cetearyl sulfate

DMBIS: S,S-dimethyl-N-(4-bromobenzoyl) iminosulfurane

DMSO: Dimethyl sulphoxide

DSC: Differential scanning calorimetry

DTA: Differential thermal analysis

HSC: Human stratum corneum

MTDSC: Modulated temperature differential scanning calorimetry

PEG: polyethylene glycol

PG: Propylene glycol

PSC: Porcine stratum corneum

SC: Stratum corneum

TGA: Thermogravimetric analysis

Graphical abstract

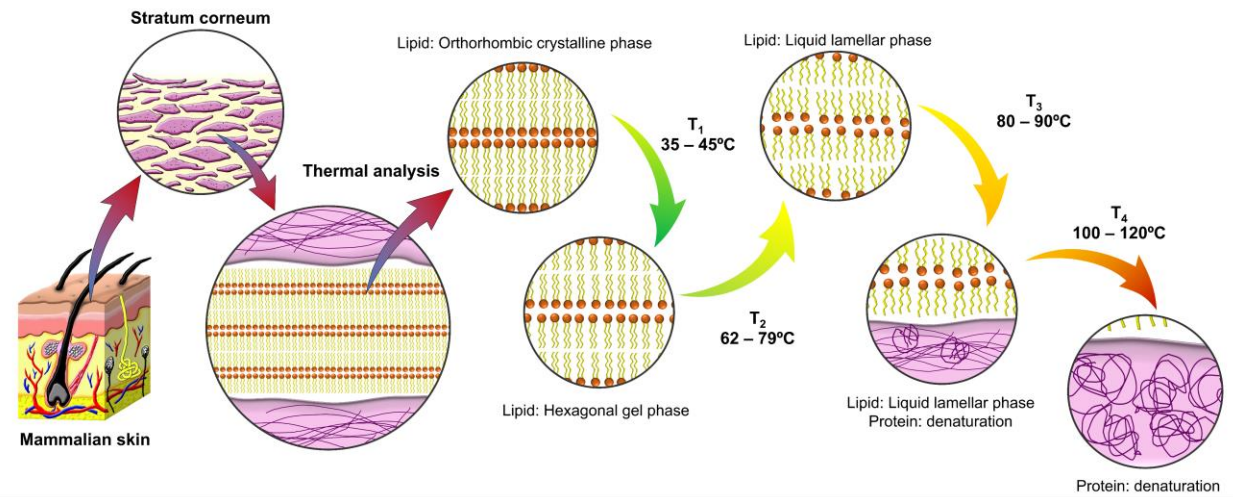

1. Introduction

In the 1970's, thermal analysis became popular among researchers investigating the functional properties of the skin. The early development of thermal analysis began with the introduction of differential thermal analysis (DTA) and this was later replaced by differential scanning calorimetry (DSC). Both analytical methods were based on the same principle, namely measuring the temperature difference between a sample and a reference.

As early as 1967, the application of thermal analysis in skin research was reported by Bulgin and Vinson (1967). This DTA work focused on the detection and characterisation of the structure of water found in human and rat stratum corneum (SC). Subsequently, the investigation of thermal transitions in human SC (HSC) was reported by Duzee (1975), following the work by Bulgin and Vinson (1967) and Walkley (1972) where bound water was detected in the SC. With these findings, thermal analysis became more widely used as a tool in skin research because of the association of thermal events with skin integrity and barrier function. In the late 1990s, four major endotherms (T_1 – T_4) were identified by Tanojo et al. (1999) as the primary thermal transitions in the DSC profiles of HSC samples. Among these four endothermic transitions, the first two lipid-related transitions (T_1 and T_2) at 40°C and 70°C are reversible or appear in the reheating cycle. The other transitions (T_3 and T_4) at 80°C and 100°C, however, are associated with protein denaturation and are irreversible but the T_3 transition also shows the involvement of lipids. Apart from these four transitions, a further transition (T_x) occurs around 55°C but is not well characterised (Gay et al., 1994). Of the four major transitions, only T_2, T_3 and T_4 have been detected in porcine SC (PSC).

Despite the wide use of thermal analysis for providing new insights into skin behaviour, the influence of experimental and instrumental variables including SC isolation and preparation methods, pan type, hydration state of the SC, heating rate and sample size is not well understood. Understanding how these parameters affect the thermal transitions of the SC is of utmost importance to gain an accurate understanding of the thermotropic behaviour of SC lipids and protein examined.

Thermal analysis with DSC has been used to explore the underlying actions of excipients, especially co-solvents and lipophilic materials. The application of DSC to advance the understanding of skin subjected to different treatments and storage conditions has also been explored. In many cases, such effects can be evaluated by monitoring the changes in the transition temperatures and enthalpies during these experiments.

In this review, we aim (i) to provide a comprehensive summary of the thermal transitions of the SC reported to date; (ii) to review the experimental and instrumental variables used in DSC analysis of the SC; and (iii) to highlight the application of DSC in advancing skin research. The present review focuses on reports using human and porcine tissue as the latter is the closest model to man. Also, the scope of thermal analytical methodology considered is largely DSC because of the extensive literature available concerning this approach. Investigation of isolated/extracted skin lipids and proteins is beyond the scope of this review.

2. Thermal transitions of the SC

A summary of thermal analytical studies of HSC and PSC, primarily using DSC, and the associated experimental and instrumental variables, is provided in Table 1 and Table 2.

Table 1 Summary of thermal analysis studies of human SC

Type of thermal analysis	Pan type	Heating rate (°C/min)	Temperature range (°C)	Sample size (mg, otherwise specified)	Average transition temperature (°C), enthalpy (J/g) in square brackets where reported					Reference
					T_1	T_x	T_2	T_3	T_4	
Dehydrated samples										
DSC	Hermetically sealed pan	20	-50 – 170	6 cm^2	50 – 150 (50 – 100[c]) (broad and multiple peaks)					Duzee (1975)
DSC	Aluminum pan	10	-20 – 140	4	-	-	77	88	-	Goodman and Barry (1986)
DSC	-	0.6	10 – 110	15 – 25	43	55	70	85[e]	-	Gay et al. (1994)
DSC	Steel pan (120 µL)	2	-10 – 130	10 – 20	-	-	75	85	105	Leopold and Lippold (1995)
DSC	Hermetically sealed stainless-steel capsule	10	0 – 140	10	41.1	57.2	73.4 (72.3[c])	86.1	-	Al-Saidan et al. (1998)
DTA	Hermetically sealed medium pressure stainless steel crucible	2	-130 – 120	10 – 30	40	-	70	80	-	Tanojo et al. (1994, 1997); Tanojo et al. (1999)
Hyper-DSC	Aluminum pan (10 µL)	100, 200, 400	-170 – 160	2 – 9	49	52 – 60	76 – 78	83 – 89	91 – 102[a]	Silva et al. (2006a); Silva et al. (2006b)
DSC	Aluminum crucible	10	25 – 350	10	-	-	68 – 78	90 – 100	105 – 120	Park et al. (2008)
DSC	Hermetically sealed aluminum pan	10	0 – 120	-	-	-	75	90	-	Kim et al. (2007); Kim et al. (2008)
DSC	Aluminum pan (40 µL)	10	5 – 160	10 – 20	-	-	63	82	99.5	Kaushik and Michniak-Kohn (2010)
DSC	Hermetically sealed pan	10	0 – 140	3 – 5	56.1 ± 2.1	-	75.6 ± 0.7 (72.8 ± 0.6 [c])	86.4 ± 0.2	125.3 ± 3.7	Unpublished work
DSC	Hermetically sealed pan	2	0 – 140	3 – 5	44.5 ± 1.7	-	71.7 ± 0.5 (70.1 ± 1.9 [c])	83.4 ± 0.6	114.3 ± 7.2	Unpublished work
MTDSC	Pinhole pan	2 (modulation amplitude of ± 1°C and a period of 60 s)	0 – 140	3 – 5	-	-	73.3 ± 0.4 (67.1 ± 0.8[c])	89.0 ± 0.3	-	Unpublished work

MTDSC	Hermetically sealed pan	2 (modulation amplitude of ± 1ºC and a period of 60 s)	0 – 140	3 – 5	46.5 ± 1.8	-	70.7 ± 0.5 (67.3 ± 0.6[c])	83.2 ± 1.3	118.8 ± 3.3	Unpublished work
Hydrated samples										
DTA	Open pan	20	30 – 140	-	-	-	70[c]	-	110	Wilkes et al. (1973)
DSC	Hermetically sealed pan	20	-50 – 170	6 cm^2	40[c]	-	75[c]	85 (90[a])	107	Duzee (1975)
DSC	-	0.5 or 0.75	25 – 105	20[b]	-	-	65 – 70	75 – 80	95 – 100[a]	Knutson et al. (1985)
DSC	-	0.5 or 0.75	25 – 105	20	35[c, d]	-	65[c]	80	95	Golden et al. (1986)
DSC	Aluminum pan	10	-20 – 140	4	38	-	72	85	102	Goodman and Barry (1986)
DSC	Glass-lined cell	0.25	0 – 100	-	28	51 – 60	75	-	-	Rehfeld et al. (1988)
DTA	Hermetically sealed pan	2	0 – 120	20	40[d]	-	70	85 [Total T_2 and T_3: 6.5]	110[d]	Bouwstra et al. (1989)
DSC	Aluminum pan (50 µL)	10	30 – 105	14	-	-	73.1[c]	85.4[c]	101.4	Khan and Kellaway (1989)
DTA	Hermetically sealed pan	2	0 – 120	20	37	-	70	85 [Total T_2 and T_3: ~6.5]	107	Bouwstra et al. (1991a)
DSC	-	10	-50 – 140	9	36	-	74	84	99	de Vos and Kinget (1993)
DSC	-	0.6	10 – 110	15 – 25	35.9	55 variable	70	80[e]	90[e]	Gay et al. (1994)
DTA	Hermetically sealed medium pressure stainless steel crucible	2	-130 – 120	10 – 30	40	-	70	80 – 85	100	Tanojo et al. (1994, 1997); Tanojo et al. (1999)
DSC	Hermetically sealed stainless steel capsule (75 µl)	10	10 – 140	8 – 12	37 – 38	-	71 – 72 [4.46 – 10.1]	83 [4.53 – 7.35]	98 – 100	Yamane et al. (1995a, 1995b)
DSC	Hermetically sealed stainless steel capsule (75 µL)	10	-10 – 140	10	36 [0.8]	51 [1.2]	72[c] [5.3]	83 [4.1]	100[a] [5.1]	Cornwell et al. (1996)

DSC	Hermetically sealed aluminum pan	2	10 – 140	20	-	-	62, 65	78, 79	95, 97	Vaddi et al. (2002a); Vaddi et al. (2002b); Vaddi et al. (2003)
DSC	Hermetically sealed stainless steel sampling cup	10	10 – 140	6 – 11	39 – 45 (not clear)	-	72	82 – 84	-	Sznitowska et al. (2003)
DSC	Aluminum pan	5	-20 – 140	-	-	-	72.4, 71.1	79.4, 81.3	-	Winkler and Müller-Goymann (2005)
Hyper-DSC	Aluminum pan (10 µL)	100, 200, 400	-170 – 160	2 – 9	40 – 49	50 – 60	68 – 79	79 – 89	91 – 109[a]	Silva et al. (2006a); Silva et al. (2006b)
DSC	Aluminum pan	5	-20 – 140	12	-	-	68.61, 65.23	80.28, 75.29	-	Mitriaikina and Muller-Goymann (2007)
DSC	Hermetically sealed platinum pan	2	20 – 110	20	-	-	53.2	78.1 – 84.1	-	Ibrahim and Li (2010)
DSC	Hermetically sealed aluminum crucible	5	20 – 120	12	-	-	70.81 ± 0.51	83.51 ± 0.73	-	Täuber and Müller-Goymann (2015)
DSC	Hermetically sealed pan	10	0 – 140	3 – 5	55.9 ± 1.3	-	75.2 ± 1.0 (64.8 ± 7.5 [c])	86.2 ± 0.2	128.5 ± 1.8	Unpublished work
DSC	Hermetically sealed pan	2	0 – 140	3 – 5	43.8 ± 3.9 (31.0 ± 1.4 [c])	-	71.3 ± 0.2 (69.0 ± 0.5 [c])	82.9 ± 0.2	107.6 ± 4.6	Unpublished work
MTDSC	Pinhole pan	2 (modulation amplitude of ± 1ºC and a period of 60 s)	0 – 140	3 – 5	-	-	71.5 ± 2.1 (63.8 ± 3.9[c])	88.3 ± 1.0	-	Unpublished work
MTDSC	Hermetically sealed pan	2 (modulation amplitude of ± 1ºC and a period of 60 s)	0 – 140	3 – 5	44.9 ± 1.3 (30.3 ± 1.5 [c])	-	69.1 ± 0.6 (63.8 ± 3.9[c])	81.7 ± 1.2	107.2 ± 2.0	Unpublished work

DSC: differential scanning calorimetry; DTA: differential thermal analysis; MTDSC: modulated temperature DSC

[a] present in delipidised samples; [b] dry sample weight with additional up to 1 mg water/mg sample; [c] present in reheating cycle; [d] not present in all samples; [e] data estimated from DSC profiles

Table 2 Summary of thermal analysis studies of porcine SC

Type of thermal analysis	Pan type	Heating rate (ºC/min)	Temperature range (ºC)	Sample size (mg)	Average transition temperature (ºC), enthalpy (J/g) in square brackets where reported				Reference
					T_1	T_2	T_3	T_4	
Dehydrated samples									
MTDSC	Pinhole pan	2 (modulation amplitude of ± 1ºC and a period of 60 s)	0 – 200	3 – 5	-	67.1 ± 0.5 (61.2 ± 0.8[c])	73.4 ± 1.0	-	Unpublished work
MTDSC	Hermetically sealed pan	2 (modulation amplitude of ± 1ºC and a period of 60 s)	0 – 200	3 – 5	-	- (64.5 ± 0.4[c])	75.3 ± 0.5	105.6 ± 1.5	Unpublished work
Hydrated samples									
DSC	-	0.5 or 0.75	25 – 105	20[b]	-	60 – 65	70 – 75	95 – 100[a]	Knutson et al. (1985)
DSC	-	0.75	25 – 120	10	-	60	70	95	Golden et al. (1987a)
DSC	-	0.75	25 – 105	20	-	65	75	105	Golden et al. (1987b)
DSC	-	0.75	35 – 110	15 – 20	-	60 [1.67]	73 [1.34]	100	Francoeur et al. (1990)
FTIR/DSC	KBr disc	2	25 –165	-	-	65 – 80[c]	65 – 80 (78[c])	115	Lin et al. (1996); Lin et al. (1994)
DSC	Aluminum crucible (40 µL)	5	0 – 100	3 – 5	-	63.0 ± 2.6	81.0 ± 2.4	-	Zhang and Lunter (2018)
MTDSC	Pinhole pan	2 (modulation amplitude of ± 1ºC and a period of 60 s)	0 – 140	3 – 5	-	- (63.8 ± 1.1[c])	68.4 ± 0.6	77.1 ± 1.0	Unpublished work
MTDSC	Hermetically sealed pan	2 (modulation amplitude of ± 1ºC and a period of 60 s)	0 – 140	3 – 5	-	- (62.3 ± 1.0[c])	71.8 ± 2.2	101.7 ± 4.8	Unpublished work

DSC: differential scanning calorimetry; DTA: differential thermal analysis; MTDSC: modulated temperature DSC

[a] present in delipidised samples; [b] dry sample weight with additional up to 1 mg water/mg sample; [c] present in reheating cycle

The first transition (T_1) is a small endothermic peak with an enthalpy value (ΔH) of 0.8 J/g (Cornwell et al., 1996) and is closely related to lipid melting (Duzee, 1975; Wilkes et al.,

1973). This transition has usually been reported in the temperature range of 35 – 45°C. However, this transition was found only in HSC but does not appear clearly and consistently (Al-Saidan et al., 1998; Bouwstra et al., 1989; Duzee, 1975; Rehfeld et al., 1988; Sznitowska et al., 2003; Yamane et al., 1995a). The inconsistent occurrence of this transition in HSC was initially thought to be a result of the poor association of the sebaceous lipids on the surface of the SC samples or sample contamination (Golden et al., 1986; Golden et al., 1987a). This hypothesis was then proven incorrect because of the detection of this transition even after the removal of surface lipids with cold hexane (Cornwell et al., 1996; Duzee, 1975; Gay et al., 1994; Yamane et al., 1995a, b). The structural rearrangement of the lipid bilayers in this transition was confirmed by Bouwstra et al. (1992) using wide angle X-ray diffraction (WAXD) where a modification of the lateral packing of lipids from an orthorhombic to a hexagonal phase, i.e., from a crystalline phase to a gel phase was observed (Figure 1). Gay et al. (1994) have also suggested that this transition represents a solid-to-fluid phase change for a discrete subset of SC lipids. This endotherm, thus, could comprise of two-phase changes which occur in two different lipid subgroups. This transition has rarely been detected in reheated samples probably because of the low enthalpy of the transition (Duzee, 1975; Gay et al., 1994; Golden et al., 1986). The main lipid classes in the SC are ceramides, cholesterol, and long-chain free fatty acids. HSC and PSC are fundamentally different in composition and chemical structure especially with reference to types of ceramides (Ponec et al., 2003; Wertz and Downing, 1983a, b). The absence of the T_1 transition in PSC is not surprising and this has been confirmed because of the absence of the orthorhombic structure (Bouwstra et al., 1995; Caussin et al., 2008).

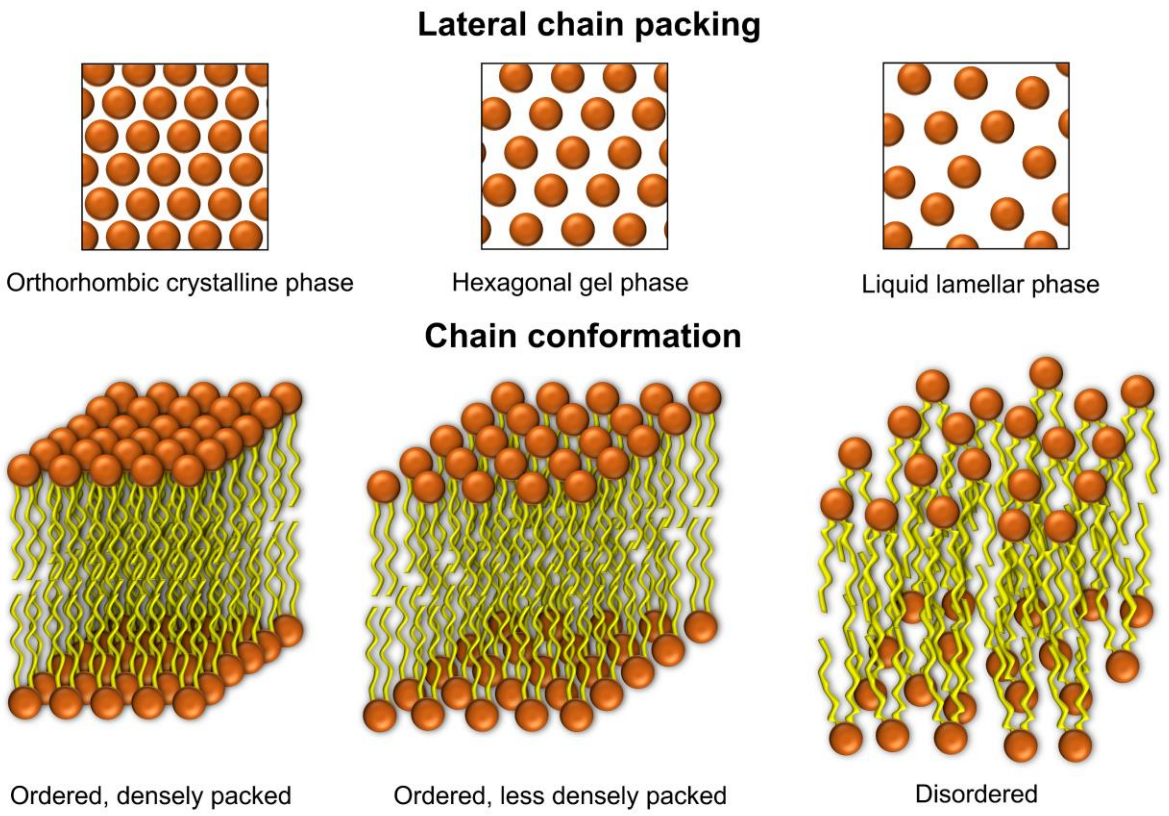

Figure 1 Lateral chain packing and chain conformation of SC lipids (adapted from Bouwstra and Gooris (2010))

As for the T_1 transition, the T_2 transition (62 – 79°C), found in both HSC and PSC, is also attributed to melting of intercellular lipids (Duzee, 1975; Golden et al., 1986; Golden et al., 1987a). This endotherm was reported to arise from the lipid domain because of its existence in the lipid extracts of both HSC (Golden et al., 1986; Goodman and Barry, 1986; Knutson et al., 1985; Leopold and Lippold, 1995; Rehfeld et al., 1988) and PSC (Golden et al., 1987a; Knutson et al., 1985). This is further substantiated by the absence of this peak in DSC profiles for delipidised HSC (Golden et al., 1986; Knutson et al., 1985; Tanojo et al., 1994, 1997; Tanojo et al., 1999; Yamane et al., 1995a, b).

Fourier transform infrared (FTIR) measurements suggested that this transition represents a modification of the conformation of the extended lamellar lipid domain within the intercellular space (Golden et al., 1986). This thermal disruption of the lipid domain was

also suggested by Knutson et al. (1985) to be related to the change of local molecular motion in the hydrocarbon chain of the lipids. This endotherm is then described as a gel-liquid transition of the lipid bilayers because of a disordering of the lamellar lipid phase observed using small-angle (SAXD) and wide-angle X-ray diffraction (WAXD) analysis as illustrated in Figure 1 (Bouwstra et al., 1991a; Bouwstra et al., 1991b; Bouwstra et al., 1992). WAXD data showed that complete loss of the lamellar structure of lipids does not occur and the hexagonal packing of the lipids still exists during this transition (Bouwstra et al., 1992).

The T_2 peak is the only transition detected following a second heating step apart from a very minor T_1 peak. The presence of the former transition in reheated samples reflects its thermal reversibility. However, there was a reduction of the enthalpy of this transition during the second heating of the same sample (Duzee, 1975; Wilkes et al., 1973). This may be related to a loss of the crystallinity of the lipid content or purely the influence of moisture loss. The T_2 peak appeared at a lower temperature in reheated samples suggested the disordering of the acyl chains of SC lipids (Khan and Kellaway, 1989). Upon first heating over 100°C, all the lipid structure was totally disrupted and, cooling before reheating, combined all the lipids into a random mixture (Goodman and Barry, 1986). This lipid mixture was shown as the T_2 peak during the second heating because of a similar transition temperature.

In between the T_1 and the T_2 transition, a further small peak (T_x) has been reported infrequently around 55°C in HSC only (Al-Saidan et al., 1998; Cornwell et al., 1996; Gay et al., 1994; Rehfeld et al., 1988; Silva et al., 2006a; Silva et al., 2006b). This transition may demonstrate a complex modification in the lattice structure of multiple lipid subsets. This shallow transition could be a disorientation or a loss of long-range alignment of crystalline orthorhombic lipid subsets (Gay et al., 1994).

The third endothermic transition (T_3), frequently reported around 80 – 90°C is the only transition involving both lipid and protein, that can be found in both HSC and PSC (Duzee, 1975; Golden et al., 1986; Golden et al., 1987a). The absence of this transition in delipidised HSC (Golden et al., 1986; Goodman and Barry, 1986; Knutson et al., 1985; Sznitowska et al., 2003; Tanojo et al., 1994, 1997; Tanojo et al., 1999) and PSC (Golden

et al., 1987a; Knutson et al., 1985) was initially reported to be related to the SC lipids. Apart from the loss of this peak upon extensive solvent extraction, a reduction of the C-H stretching vibrations of the long-chain lipids reported by FTIR analysis in the temperature range of 70 – 80°C supported the contribution of lipids to this transition (Golden et al., 1986; Golden et al., 1987a). Microscopic calorimetric work with FTIR spectroscopy also showed a dramatic increase of the asymmetric stretching mode of fatty acyl chains of PSC lipids near 2920 cm^{-1} between 65°C and 80°C (Lin et al., 1994).

The involvement of protein in this transition was previously reported by Duzee (1975) as α-keratin protein denaturation. The study also showed that this transition is thermally irreversible because it is present in the delipidised SC samples but not in the lipid extract of the SC. The same study employed ether to destroy the cell membranes of the SC and urea to denature the α-keratin inside the corneocytes. The T_3 transition was lowered in these samples, suggesting the involvement of protein in this transition. Also, the absence of this peak in the lipid extracts substantiated the attribution of this endotherm to proteins (Goodman and Barry, 1986).

Based on these results for the presence of both extractable (lipid) and non-extractable (protein) components, Golden et al. (1986) proposed that this transition actually reflects a lipid-protein complex. The lipid-protein interaction increases the ordering of SC lipids that is reflected by a positive shift of the transition midpoint of C-H stretching vibrations. The presence of protein in stabilising the lipid organisation was previously suggested by Chapman (1975) in other biological systems. These results strongly support the participation of protein in this transition but as a protein-lipid complex associated with the corneocyte membrane. Bouwstra et al. (1991a) also described this transition as a gel-to-liquid transition of lipids involving SC proteins.

Reheating shifted this peak to a smaller one shown as a single peak around T_2 (Golden et al., 1986). This shift was explained previously as all lipid content forming a random mixture upon cooling after exposure to high temperature (Goodman and Barry, 1986). When reheating the cooled sample, this consolidated lipid mixture from the T_2 and T_3 events appeared at a transition similar to the T_2 peak.

The fourth transition (T_4) is ascribed to protein denaturation in HSC (Cornwell et al., 1996; Golden et al., 1986; Goodman and Barry, 1986; Knutson et al., 1985; Yamane et al., 1995a, b) and PSC (Golden et al., 1987a; Knutson et al., 1985). This transition was also present in both delipidised HSC (Cornwell et al., 1996; Golden et al., 1986; Goodman and Barry, 1986; Knutson et al., 1985; Yamane et al., 1995a, b) and PSC (Golden et al., 1987a; Knutson et al., 1985), indicating a protein-associated transition. Duzee (1975) noted that further heating following the third transition caused the irreversible denaturation of protein on the surface of the cell membranes or in the intercellular spaces, giving rise to the T_4 transition. Because of the thermal irreversibility of this transition it was not detected following a second heating step for both HSC (Cornwell et al., 1996; Duzee, 1975; Khan and Kellaway, 1989; Pouliot et al., 1999) and PSC (Francoeur et al., 1990; Golden et al., 1987a).

Alkaline extraction of the corneocyte membrane to remove the intracellular keratin in PSC samples caused the absence of the T_4 transition (Golden et al., 1987a). In addition, a decrease in intensity of the amide I band at 1651 cm^{-1} and a redshift of the amide II band at 1543 cm^{-1} were observed when PSC was heated beyond 115°C in an in-house combined microscopic FTIR/DSC system (Lin et al., 1996). This indicated protein denaturation with conversion of α-keratin to the β form.

Overall, there are four major thermal transitions (T_1, T_2 ,T_3 and T_4) frequently reported for HSC while three of them (T_2 ,T_3 and T_4) can be found in PSC. The related changes to the skin components, SC lipids and protein are illustrated in Figure 2.

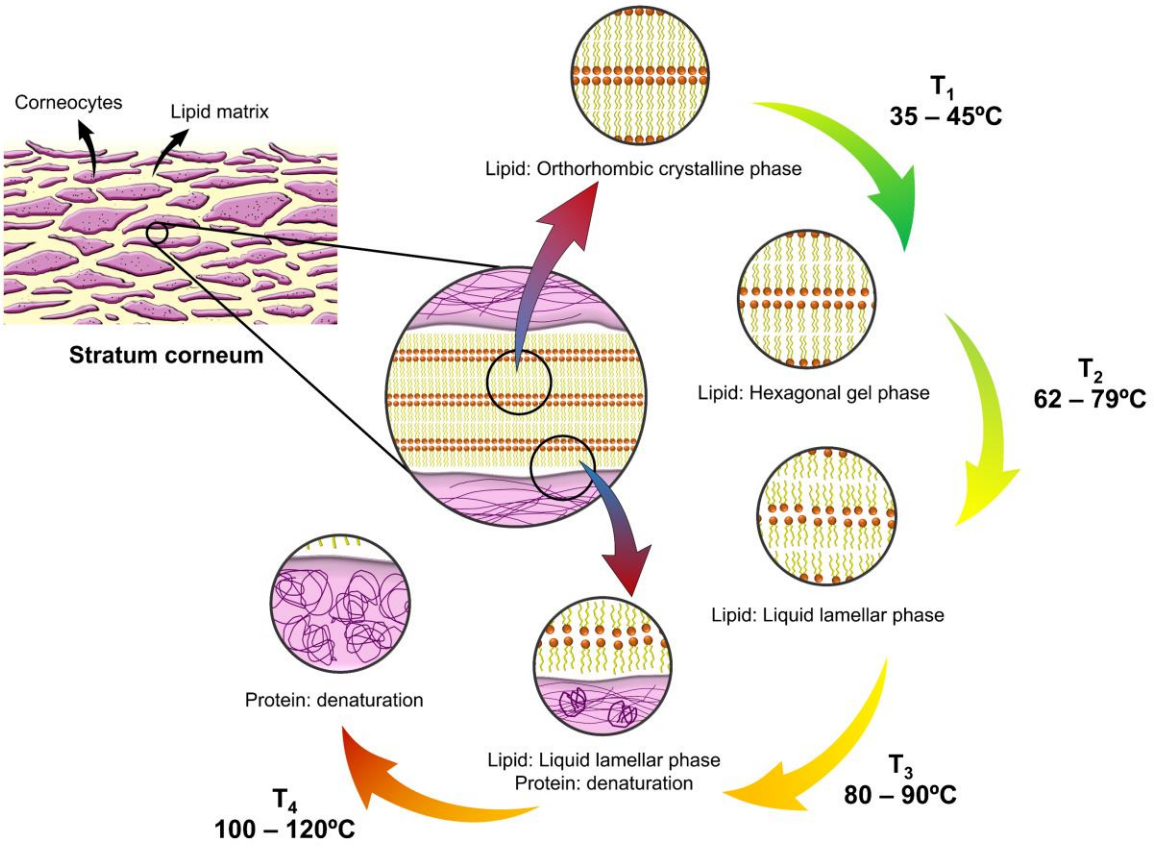

Figure 2 Illustration of stratum corneum lipid organisation and protein structure at respective thermal transitions

Apart from the lipid and protein transitions, Tanojo et al. (1994) also pioneered the investigation of subzero transitions for HSC by analysing skin samples at temperatures as low as -100°C. Dehydrated HSC demonstrated a transition at -9°C, reflecting changes in lipids. An additional peak at approximately -18°C was detected in hydrated samples and this was ascribed to the unbound water in HSC. These subzero peaks were not detected in the extracted lipids. However, it is unusual to conduct such experiments at extremely low temperatures as they do not translate into any real-world application of this technique.

3. Experimental and instrumental variables of DSC

3.1. Isolation and preparation of SC

Table 3 summarises the methods used for isolation of SC and the processes for preparing dehydrated, hydrated and delipidised SC for thermal analysis. Dermatomed and heat-separated skin samples are commonly used prior to trypsinisation to isolate the SC. A wide concentration range of trypsin solution (0.0001 – 0.5%), usually prepared in buffers such as phosphate buffer saline (PBS), has been used in previous studies. Several groups also rinsed the isolated SC with cold hexane (Duzee, 1975; Gay et al., 1994; Golden et al., 1986; Khan and Kellaway, 1989; Knutson et al., 1985) or acetone (Cornwell et al., 1996; Vaddi et al., 2002a; Vaddi et al., 2002b; Vaddi et al., 2003; Yamane et al., 1995a, b) to remove unwanted surface lipids such as sebum before drying.

Dehydrated and hydrated SC samples are typically analysed using DSC to understand the influence of water on thermotropic transitions. Various drying processes were found to dry fully the SC samples including storage with desiccants such as silica and phosphorus pentoxide (some with a vacuum) and flushing the sample with nitrogen gas. On the other hand, hydrated SC samples have been prepared by incubating dry SC samples on saturated salt solutions including ammonium chloride, ammonium phosphate, barium chloride, copper sulphate, potassium sulphate, sodium chloride, sodium bromide and sodium sulphate.

Delipidised samples have been studied to gain additional knowledge about protein-related transitions. The skin lipids are usually extracted from SC samples using organic solvents such as a mixture of chloroform and methanol.

1 **Table 3 Isolation and preparation methods for dehydrated, hydrated and delipidised SC**

Isolation of SC				Preparation of dehydrated, hydrated and delipidised SC			Reference
Isolation of epidermis	**Trypsinisation**	**Removal of surface lipids**	**Drying process (storage)**	**Dehydration**	**Hydration**	**Lipid extraction**	
Human SC							
Heat separation	0.1% trypsin solution (0.15 M sodium chloride and 0.05M Tris, pH 7.4)	Cold hexane (0°C) for 5 m	48 h over anhydrous calcium sulphate	No additional drying process	-	-	Duzee (1975)
Dermatome	0.5% trypsin solution in PBS (pH 7.4) for 1.5 h at 37°C	Cold hexane (-4°C) for 30 s	Desiccator	-	Chamber with saturated salt solution	2:1 (v/v) chloroform:methanol for 16 h	Knutson et al. (1985)
Dermatome	0.5% trypsin solution in PBS (pH 7.5) for 1.5 h at 37°C	Cold hexane (-4°C) for 30 s	Desiccator	-	0.5mg water/mg dry weight with saturated salt solution	-	Golden et al. (1986)
Heat separation	0.0001% trypsin solution overnight at 37°C	-	-	-	Over a saturated salt solution	-	Goodman and Barry (1986)
Dermatome	0.1% trypsin solution in PBS for one night at 37°C	-	Silica in a vacuum desiccator	-	Over a saturated solution of ammonium chloride	-	Bouwstra et al. (1989)
Heat separation or dermatomed epidermis	0.1% trypsin solution (0.15 M sodium chloride and 0.05M Tris, pH 7.4) for 1 h	Cold hexane (-4°C) for 1 m	48 h over anhydrous calcium sulphate	-	Over a saturated solution of barium chloride or potassium sulphate	-	Khan and Kellaway (1989)
Dermatome	0.1% trypsin solution in water for 14 h	-	Silica in a vacuum desiccator	-	Over a saturated solution of ammonium chloride or ammonium phosphate	-	Bouwstra et al. (1991a)
Heat separation	0.0001% trypsin solution containing 0.5% w/v sodium hydrogen carbonate	-	Silica gel in a closed container	-	Over a saturated solution of copper sulphate	-	de Vos and Kinget (1993)
Dermatome	0.5% trypsin solution in PBS (pH 7.4)	Cold hexane (5°C)	Nitrogen gas	No additional drying process	-	-	Gay et al. (1994)
Dermatome	0.1% trypsin solution in PBS (pH 7.4) for 24 h at 4°C and 1 h at 37°C	-	Phosphorus pentoxide at 50°C for 24 h	No additional drying process	Above a 27% w/v sodium bromide solution at room temperature for 24 h	-	Tanojo et al. (1994, 1997); Tanojo et al. (1999)

Dermis excision using scapel	0.5% trypsin solution in PBS (pH 7.4) for several hours at 37ºC	-	Silica gel	No additional drying process	-	-	Leopold and Lippold (1995)
Heat separation	0.0001% trypsin solution containing 0.5% w/v sodium hydrogen carbonate for 12 h	Acetone (ice-cold) for 10 s	Silica gel in a vacuum desiccator	-	Over a saturated solution of sodium sulphate	-	Yamane et al. (1995a, 1995b)
Heat separation	0.0001% trypsin solution containing 0.5% sodium bicarbonate for 12 h	Acetone for 20 s	Silica gel in a vacuum desiccator	-	Over a saturated solution of sodium sulphate	2:1 (v/v) chloroform:methanol for minimum 48 h	Cornwell et al. (1996)
Dermatome	0.025% trypsin solution in PBS (pH 7.4) for 10 – 12 h at 37ºC	-	Silica gel for at least 3 days	No additional drying process	-	-	Al-Saidan et al. (1998)
Heat separation	0.1% w/v trypsin solution in 0.5% w/v sodium bicarbonate for 3 h at 37ºC	Acetone for 20 s	Vacuum desiccator	-	Over a saturated solution of potassium sulphate for 3 – 4 days	-	Vaddi et al. (2002a); Vaddi et al. (2002b); Vaddi et al. (2003)
Heat separation	0.1% trypsin solution containing 0.5% sodium bicarbonate for 3 h at 37ºC	-	Silica gel in a desiccator	-	Over a saturated solution of potassium sulphate	-	Sznitowska et al. (2003)
-	2% trypsin solution for 24 h at 37ºC	-	Desiccator	-	Over a saturated solution of sodium chloride for 48 h	-	Mitriaikina and Muller-Goymann (2007); (Täuber and Müller-Goymann, 2015); Winkler and Müller-Goymann (2005)
Dermatome	0.1% trypsin solution in PBS for one night at 37ºC	-	Desiccator for 24 h	Phosphorus pentoxide at 50ºC overnight	Over a solution of 27% sodium bromide for 2 days	2 hours in 3 different chloroform:methanol systems (2:1, 1:1, 1:2) at room temperature, extraction repeated after 1 h each and extracted overnight with methanol (hydrated before use)	Silva et al. (2006a); Silva et al. (2006b)
Heat separation	0.5% trypsin solution in PBS for 12 h at 4ºC	-	Vacuum	No additional drying process	-	-	Park et al. (2008)
Heat separation	0.25% trypsin solution (0.01% gentamicin) in PBS for 24 h at 32ºC	-	Vacuum overnight at room temperature	Vacuum desiccator for 12 h	-	-	Kim et al. (2007); Kim et al. (2008)

-	0.1% trypsin solution in PBS for 4 h	-	Desiccator	-	-	-	Kaushik and Michniak-Kohn (2010)
Heat separation	0.2% trypsin in PBS for 16 h at 37ºC	-	Desiccator for 12 h	-	Equilibrate with PBS	-	Ibrahim and Li (2010)
Porcine SC							
Dermatome	0.5% trypsin solution in PBS (pH 7.5) for 1.5 h at 37ºC	Cold hexane (-4ºC) for 30 s	Desiccator	-	Over a saturated salt solution	-	Knutson et al. (1985)
Dermatome	0.5% trypsin solution in PBS (pH 7.4) overnight at 22ºC	-	Dry atmosphere	-	Over a saturated solution of sodium chloride for several days	-	Golden et al. (1987a)
Dermatome	0.5% trypsin solution in PBS (pH 7.4) for several hours at 37ºC	-	Desiccator	-	In a chamber with 95% RH and 22ºC	-	Francoeur et al. (1990); Golden et al. (1987b)
Heat separation	0.5% trypsin solution in PBS (pH 7.4) for 3 h	-	Desiccator	-	Incubated in distilled water for 24 h at 25ºC	-	Lin et al. (1996); Lin et al. (1994)
Dermatome	0.2% trypsin solution in PBS (pH 7.4) overnight at room temperature	-	Silica gel in a desiccator (at least 3 days)	-	Over a solution of 27% sodium bromide for 24 h	-	Zhang and Lunter (2018)

2

3.2. Pan type

The two common pan types for analysing thermotropic transitions of HSC are aluminum (not airtight) and hermetically sealed (airtight) pans as shown in Table 1. These pan types prevent the escape of volatile materials from the samples on heating. Duzee (1975) and Cornwell et al. (1996) reported that the seal prevents water vaporisation from the skin tissues up to and including 100ºC. It must be borne in mind that the seals are only guaranteed up to certain temperatures and pressures, even with airtight seals, and the pan may burst. There may be a large headspace above the samples which can contribute to water vaporisation within the pan itself. Sealing the pan under nitrogen gas can avoid this problem.

It is evident that the report of the T_1 transition is more consistent with the use of hermetically sealed pans for human skin samples as compared to general aluminum pans. This might suggest a strong association of vapourised materials in the SC, namely water with this lipid transition. However, there is no significant influence of the pan type on the other transitions. At present, only one report by Wilkes et al. (1973) involved the use of an open pan system to investigate the thermal behaviour of HSC. This study only reported two endotherms – the T_2 and T_4 transitions.

However, no pan type details have been reported for most PSC studies (Table 2). The influence of pan type on PSC thermal transitions cannot therefore be fully dissected but it might be expected to be similar to observations for HSC experiments.

Clearly, the selection of pan type is critical in DSC analysis, especially for transitions associated with water such as the T_1 transition. Our recent work (unpublished) compared the use of two pan types – pinhole pans and hermetically sealed pans on the thermal transitions observed with DSC at a heating rate of 2ºC/min from 0ºC to 200ºC. Pinhole pans (pans with a hole in the lid) are generally used to dry samples on heating, particularly to analyse thermal events that may be complicated by water or solvent loss. Pinhole pans usually enable water to evaporate in a controlled and repeatable manner due to the high definition of the escape route. In the unpublished work, water loss occurred at ~60ºC for both PSC and HSC samples. This means water is removed completely from the SC during

the first heating step. From our observations, analysis with pinhole pans reveals only a broad water loss endotherm. On reheating in the same temperature range, there is only one transition reported that is ascribed to the T_2 lipid transition.

On the other hand, hermetically sealed pans maintain the hydration level of SC samples. These pans allow water to evaporate at a higher temperature (around the boiling point of water, 100ºC) for PSC samples. For HSC, we obtained a typical DSC curve as reported in the literature where all four major transitions are present in the curve. The reappearance of the T_2 transition was observed to be sharper and also had a larger enthalpy as compared to that analysed using the pinhole pan during reheating (in the same temperature range). Therefore, this gel-liquid transition of the lipid bilayers (T_2) is clearly influenced by the presence of water. This also explains the importance of water in the SC lipids. Duzee (1975) suggested that water increases the order of the lipid crystal lattice as observed for other lipid systems such as myelin, as reported by Ladbrooke and Chapman (1969). Golden et al. (1986) proposed that an extensive network of hydrogen bonding between water molecules and the polar head groups of lipids increases the sharpness of the lipid transition. Since there is a strong association between pan type on the thermal behaviour of SC with hydration status, further discussion of this topic is continued later in this review.

3.3. Sample size

A wide range of sample weights has previously been used for studying the thermal behaviour of SC from as low as 2 mg to a mass of 20 times this value. Typically, a sample mass of 10 – 20 mg is preferred. The selection of a high sample mass may be a function of the nature of the sample i.e. biological tissues such as skin. During a melting event of a standard sample such as a drug substance in DSC, a high sample size requires more heat supply for the sample to melt and a larger and sharper peak is expected. This increases the sensitivity of the analysis, but the resolution will be compromised. Depending on the pan size, loading the skin tissues into a confined space can be very challenging because they are light and tend to occupy a high volume. We attempted to

introduce more than 5 mg of SC into a 40 μL pan but failed. Even though a high sample mass may be preferred for biological tissues, the sample contact with the bottom of the pan is also important to establish a good thermal contact between the sample and the instrument for a uniform temperature distribution. Our own experience is that a reasonably good and reproducible DSC profile can be obtained by using 3 – 5 mg of samples (with multiple folding) which is similar to the typical sample size for drug analysis.

3.4. Heating rate and calorimetric mode

Heating rate has been reported to have a significant influence on the resolution of a DSC curve. A higher heating rate should have a negative impact on the resolution but this may shorten the analytical time. In investigations of drug substances using DSC, a heating rate of 10ºC/min has been a recommended starting point (Lever, 2007). As shown in Table 1 and Table 2 most reports in the 1980s used this heating rate. A slower heating rate such as 0.25, 0.5, 0.6, 0.75 and 2ºC/min was employed in later reports, probably because of poor resolution of the DSC profiles using the higher heating rate. However, a slower heating rate may be accompanied by reduced sensitivity.

To date, only one study has investigated SC samples using Hi-speed DSC at 100, 200 and 400ºC/min (Silva et al., 2006a). In this study, second derivatives of the obtained DSC curves were used to detect four additional subtle transitions. Given the complexity of skin tissue, there are possibilities to detect transitions derived from components other than skin lipids and protein. However, the use of second derivatives in data interpretation may be misleading because the background noise can be greatly enhanced.

Reproducibility of DSC curves has been highlighted in the past as a major hurdle to detect consistently the transitions, especially those with a low enthalpy such as the T_1 transition. This, however, is related to the sensitivity and resolution issues. Vaddi et al. (2003) proposed the use of a slower heating rate to resolve this problem. Although a heating rate as low as 0.25ºC/min has been employed in some investigations, the experiments can be time consuming.

We attempted to explore two heating rates (2 and 10ºC/min) to analyse HSC. The SC sheets were separated by trypsinisation and dehydrated SC was prepared by storing in a closed vessel over phosphorus pentoxide for 24 h at 50ºC (Tanojo et al., 1994; Tanojo et al., 1999). While hydrated SC was prepared by keeping in a closed vessel over sodium bromide (27% w/v) solution for 24 h at room temperature (Tanojo et al., 1994; Tanojo et al., 1999). The samples were analysed in a nitrogen atmosphere at a flow rate of 50 mL/min using a modulated temperature differential scanning calorimeter (DSC Q1000, MTDSC; TA instruments, Leatherhead, UK) equipped with a refrigerated cooling system. The detailed experimental and instrumental variables can be found in Table 1. In this attempt, the transitions can be detected clearly with a more defined peak shape and a higher resolution at a lower heating rate as shown in Figure 3 (data can be found in Table 1). However, a flat baseline is still difficult to attain at this heating rate. Modeling the DSC profiles may be used to address the baseline correction (Sandu and Singh, 1990) but too much data manipulation may result in erroneous interpretation.

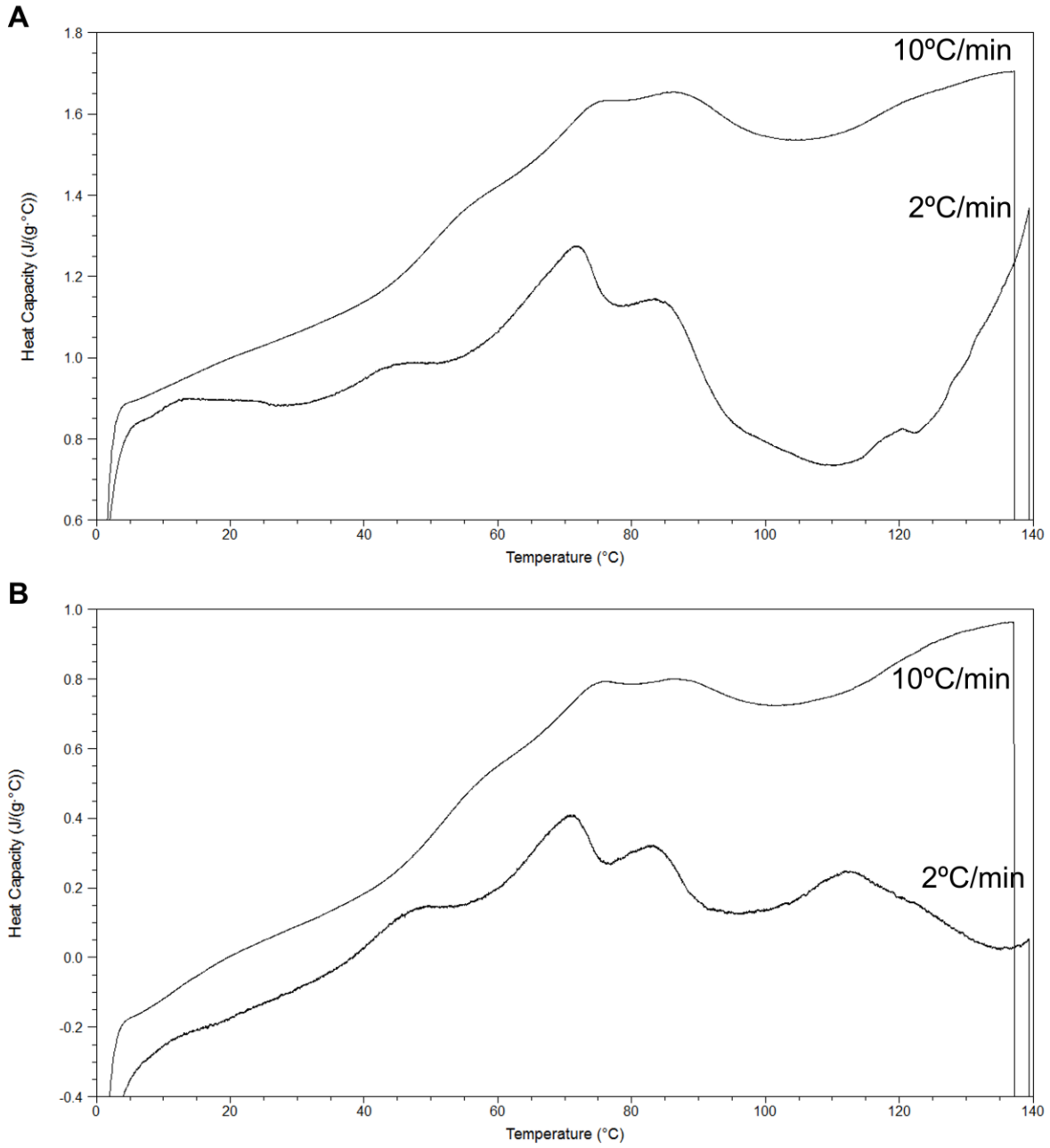

Figure 3 DSC curves of (A) dehydrated and (B) hydrated HSC at different heating rates (2 and 10ºC/min) using hermetically sealed pans (unpublished work)

Apart from conventional DSC analysis, we also attempted a modified form of DSC, modulated temperature DSC (MTDSC), for thermal investigation of skin that allows temperature to be modulated slowly during sample analysis. In brief, the usual heating and cooling programs in MTDSC are perturbed by a modulation (e.g. a sine wave in the case of the TA Instruments model), followed by mathematical deconvolution of the calorimetric response, using a Fourier transform method for both linear and modulated temperature programs (Coleman and Craig, 1996). The general heat flow signal is expressed as the sum of two different responses, the 'kinetic' and 'heat capacity' responses in conventional DSC. MTDSC is able to separate the two responses and records them as different signals – reversing and non-reversing signals. A reversible heat capacity event recorded in the reversing signal is proportional to the rate of change of temperature. The non-reversing signal dictates the irreversible kinetically controlled phenomena (chemical or physical reactions) that are dependent on the absolute temperature. The reversing heat flow is usually reversible where the process may be reversed by a minor modification of a variable. This process usually absorbs or radiates heat in the DSC instrument to match the temperature program or to achieve equilibrium with the surroundings. The non-reversing heat flow is irreversible for a chemical reaction that is kinetically controlled and not in equilibrium with the temperature program (Coleman and Craig, 1996). This heat flow signal is then expressed as:

$$\frac{dQ}{dt} = C_p \frac{dT}{dt} + f(t,T) \qquad \textbf{Equation 1}$$

where Q is the heat, C_p is the 'thermodynamic' heat capacity caused by the energy stored in vibrations, rotations and translations of molecular constituents of the sample, T is the absolute temperature and $f(t,T)$ is the calorimetric response of any kinetically controlled chemical or physical phenomenon as a function of time and temperature. A mathematical algorithm, namely a Fourier transform, can be applied in this situation to deconvolute the heat flow signal based on the two distinctive temperature programs (linear and modulated). The reversing heat flow component attributed to the cyclical heat flow is determined based on the multiplication of the C_p and the underlying heating rate. The subtraction of this reversing component from the total heat flow results in a further component called non-reversing heat flow.

With the power of deconvolution, the MTDSC curve of the SC, be it dehydrated or hydrated, obtained using pinhole pans showed a clear separation of the peak of water evaporation from the thermal transitions of PSC (Figure 4A) and HSC (Figure 4B), showing mainly T_2 and T_3 transitions. The detailed experimental and instrumental variables are similar as previously described for conventional DSC analysis and further details (together with the data) can be found in Table 1 and Table 2. These transitions were masked by a large endothermic peak of water evaporation as observed in the total heat flow signal during the first heating cycle. From the reversing signal, two distinct transitions (T_2 and T_3) were observed during the first heating cycle. The dehydration process was observed as a large endothermic peak in the non-reversing signal.

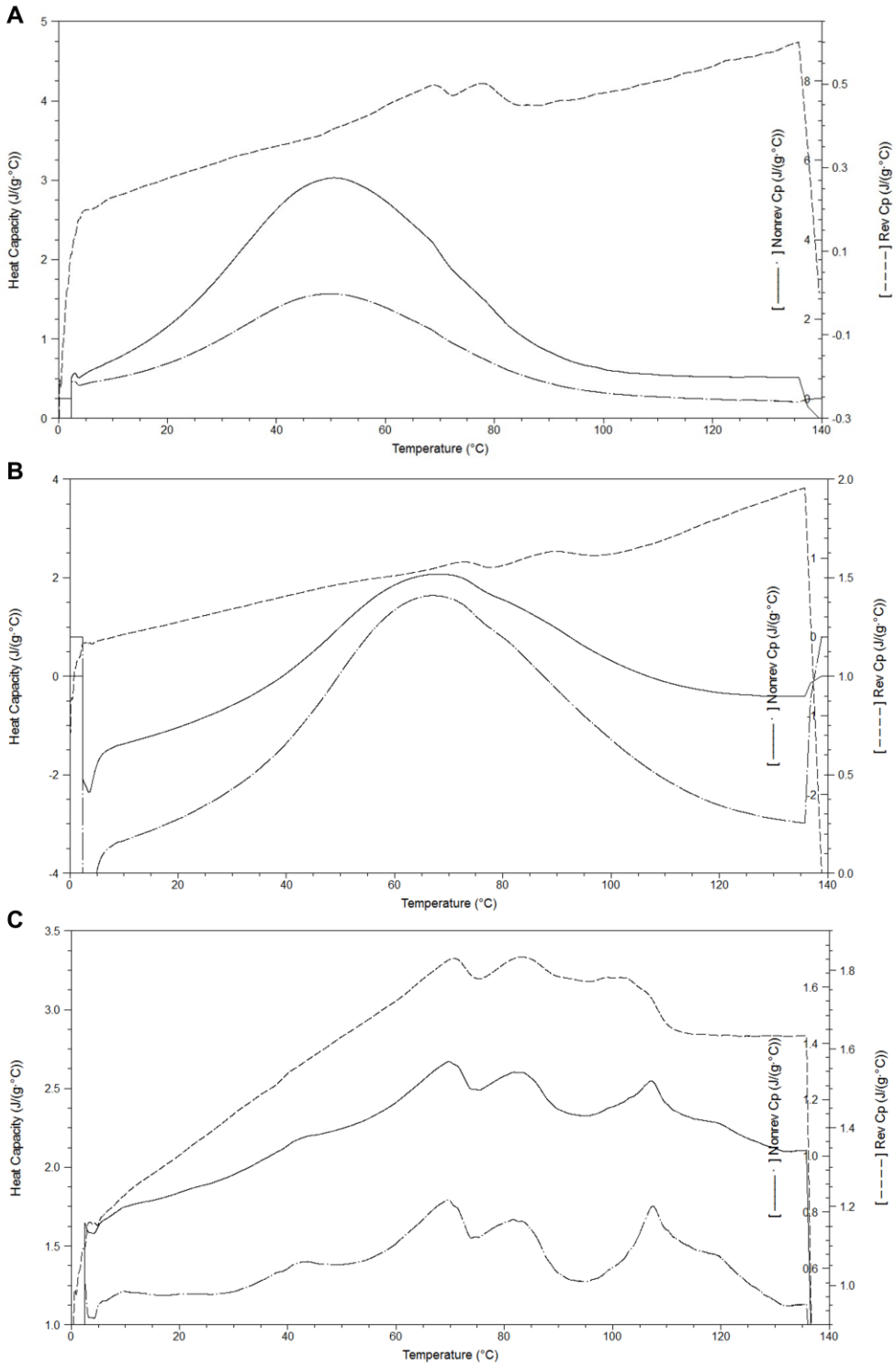

Figure 4 MTDSC curves of hydrated (A) PSC and (B – C) HSC (heating rate: 2ºC/min, modulation amplitude: ± 1ºC, period: 60 s) showing the total heat capacity (——), reversing (– – –) and non-reversing (– • –) signals (first heating cycle) using (A – B) pinhole pans and (C) hermetically sealed pans (unpublished work)

MTDSC runs showed no major difference from conventional DSC for HSC using hermetically sealed pans (Figure 4C). All four thermal transitions of HSC were recorded in the non-reversing signal during the first heating step (data can be found in Table 1 and Table 2). Notwithstanding this, we noticed a sharper T_1 transition in the reversing signal in the reheating cycle that was not detected clearly in conventional DSC in our study nor in previous reports. This transition was reported to involve a very low enthalpy and was observed as a small endotherm (Cornwell et al., 1996; Duzee, 1975; Gay et al., 1994). Therefore, we believe that MTDSC is a powerful approach for detection of transitions with a low enthalpy such as the T_1 transition.

3.5. Hydration status of the SC

Gay et al. (1994) and Silva et al. (2006a) previously reported that the skin hydration level does not have a major effect on the thermal behaviour of HSC. However, several reports revealed that sharper peaks for lipid-associated transitions (T_2 and T_3) were generally observed in hydrated HSC indicating the role of water in maintaining the highly ordered lipid crystal lattice (de Vos and Kinget, 1993; Duzee, 1975; Golden et al., 1986; Goodman and Barry, 1986). A sharper endothermic T_3 peak was explained as the formation of an extended lipid network because of hydrogen bonding between the polar head group of the intercellular lipids and water (Barry, 1987). A similar observation was also reported when hermetically sealed pans were used where water content remains in the skin samples.

Apart from the influence of hydration on the major lipid endotherms, the protein peak (T_4) is also greatly affected by the presence of water. Water content is the key in determining the proper function of protein in the skin as described by Duzee (1975). This transition is not usually detected in dehydrated HSC (Al-Saidan et al., 1998; Gay et al., 1994; Goodman and Barry, 1986; Leopold and Lippold, 1995; Park et al., 2008; Tanojo et al., 1994, 1997; Tanojo et al., 1999). Protein denaturation occurring during this transition reflects the interaction between protein and water. Heating causes the loss of bound water in the SC (Duzee, 1975). The absence of this peak in dehydrated and delipidised

HSC as observed by Tanojo et al. (1994) has also underlined the importance of water-protein interactions.

The effect of hydration on the low-temperature lipid transition (T_1) has not been widely explored to date but Bouwstra et al. (1991a) claimed that at least 15% of water content is needed to allow the detection of this transition. Our unpublished work confirms the absence of the T_1 transition in the reheating cycle of dehydrated HSC (Figure 3A) and its presence in both heating cycles of hydrated HSC using hermetically sealed pans. This strongly suggests the involvement of water in lateral lipid packing during this T_1 transition. Further investigation of water content in the SC using thermogravimetric analysis (TGA) confirmed that dehydrated SC samples contain a residual amount of water. Theoretically, dehydrated SC should not contain any water as it is expected to be fully dry at 50ºC after 24 h. This is in good agreement with the observation reported by Park et al. (2008). The most tightly-bound water molecules are still present in dehydrated SC samples (Mak et al., 1991). This also explains the presence of the T_1 transition only in the first heating cycle of dehydrated HSC. Even though the water peak was not shown in the second heating cycle of the DSC runs, a small water loss fraction was still reported using TGA. This loss likely reflects the tightly bound water molecules that were not completely removed during the first heating cycle. Because of the presence of only a minimal amount of tightly-bound water in the reheating cycle, the T_1 transition was not detected for dehydrated HSC samples.

To date, no investigation of the hydration effect on the thermal transitions of PSC has been reported as the literature only reports data for hydrated PSC samples. Our unpublished results also show that there is no major difference found in the thermal transitions observed for PSC samples of different hydration statuses.

4. Applications of DSC in advancing topical and transdermal drug delivery

The use of thermal analysis in skin research is not confined solely to understanding the thermotropic behaviour of the SC. Since the introduction of thermal analysis and specifically DSC, the technique has been employed to investigate the changes of thermal

transitions and enthalpies after certain treatments of the skin, including the application of excipients commonly used in topical and transdermal formulations.

DSC has been used extensively to deduce the action of excipients in modifying drug delivery through the skin. This is usually achieved by monitoring modifications of thermal transitions and enthalpies. Table 4 and Table 5 summarise the comparisons of thermal transitions of HSC and PSC, respectively, after the application of selected excipients including propylene glycol (PG), dimethyl sulphoxide (DMSO), ethanol, fatty acids and terpenes. The proposed actions of these excipients on various skin components are also included. Most of the transitions reported, especially the lipid peaks (T_2 and T_3) have a lower temperature compared with untreated samples. Goodman and Barry (1986) explained the lipid peaks at lowered temperatures, after treatment of HSC with 60% of DMSO and above, as related to increased lipid fluidity (less ordered state). There is also a complete disappearance of the lipid peaks after treatment with Azone™ that may indicate complete lipid fluidisation (Goodman and Barry, 1986). The extent of lowering of lipid peaks (lipid fluidisation) was speculated to be indicative of the strength (potency) of the excipients in increasing drug permeation in the skin. Golden et al. (1987b) observed that an increased skin flux of salicylic acid was accompanied by a reduction in the T_2 transition of PSC after treatment with several long-chain fatty acids. Likewise, the changes to the protein peak (T_4) including a reduction in the peak magnitude, peak broadening and disappearance were related to potential actions of the excipient on the skin that would alter drug transport. The extent of the peak distortion was also hypothesised to reflect the ability of the excipient to perturb skin proteins (Khan and Kellaway, 1989).

Table 4 Modification of human SC transition temperatures following treatment with selected excipients and formulations used in topical and transdermal formulations

Excipient/Formulation	Transition temperature (ºC), enthalpy (J/g) in square brackets where reported					Proposed actions	Reference
	T_1	T_x	T_2	T_3	T_4		
Untreated	38	-	72	88	99	-	Goodman and Barry (1986)
DMSO (20%)	39/40	-	72	86	94	Lipid fluidisation, protein denaturation	
DMSO (40%)	39	-	72	85	-		
DMSO (60%)	40	-	70	83	-		
DMSO (80%)	-	-	66	76	-		
DMSO (100%)	-	-	56	66	-		
Azone™ (3% in 0.1% Tween 20)	-	-	-	-	99	Lipid fluidisation	
Untreated	40	-	70	85 [Total T_2 and T_3: 6.5]	110	-	Bouwstra et al. (1989)
PG	-	-	65	77 [Total T_2 and T_3: 7.2]	-	Reduced water hydration of the SC	
Azone™ C6	-	-	60	75 [Total T_2 and T_3: 6.9]	-	Increased mobility of alkyl chains in the lipid bilayers, reduced water hydration of the SC	
Azone™ C12	-	-	-	70 [Total T_2 and T_3: 3.3]	-		
Azone™ C16	-	-	-	65 [Total T_2 and T_3: 2.9]	-		
Untreated	-	-	73.1	85.4	101.4	-	Khan and Kellaway (1989)
DMSO (70%)	-	-	74	86, 89	-	Delipidisation, protein denaturation	

DMSO (90%)	-	-	75	90	-		
DMSO (100%)	-	-	-	92	-		
Untreated	36	-	74	84	99	-	de Vos and Kinget (1993)
Cetiol® HE (polyoxyethylene-(7)glyceryl monococoate) (10%)	38	-	-	81	94	Insertion into skin lipids, disruption of lipid packing	
Eumulgin® B3 (polyoxyethylene(30)cetostearyl ether) (10%)	37	-	74	84	95	No effect	
Cetiol® HE (10%)/ Eumulgin® B3 (10%)	37	-	73	84	95	No effect	
Untreated	37 – 38	-	70 – 75 [4.46 – 10.1]	83 – 87 [4.53 – 7.35]	98 – 100	-	Yamane et al. (1995a)
Oleic acid (5% in PG)	-	-	58.3 – 59.1 [3.53 – 7.19]	69.9 – 71.2 [5.74 – 8.34]	-	Disruption of lipid bilayers, tissue (protein) dehydration	
d-Limonene	-	-	49.1 – 50.7 [4.9 – 7.61]	65.8 – 66.6 [4.08 – 6.4]	~110 (broadened)		
1,8-Cineole	-	-	47.5 – 51.1 [2.43 – 5.8]	68.4 – 70.9 [2.05 – 7.3]	~110 (broadened)		
Menthone	-	-	50.7 – 51.5 [7.35 – 10.2]	70.7 – 71.5 [8.24 – 10.4]	-		
Nerolidol	-	-	68.9 – 70.5 [7.85 – 13.5]	80.1 – 82.3 [6.26 – 11.3]	-		
Untreated	38.1 [1.91]	-	70.9 [6.65]	83.2 [5.88]	98.1 [7.09]	-	Yamane et al. (1995b)

PG (90%)	39. 5 [2.05]	-	67.7 [5.96]	75.7 [5.37]	102.7 [8.95]	Lipid disruption/fluidisation	
d-Limonene (saturated in 90% PG)	-	-	45.1 [5.42]	61.8 [4.39]	n.s.c.	-	
1,8-Cineole (saturated in 90% PG)	-	-	42 [2.54]	58.1 [3.42]	n.s.c.	Lipid disruption/fluidisation	
Menthone (saturated in 90% PG)	-	-	52.8 [3.1]	62.3 [5.09]	n.s.c.	Lipid disruption/fluidisation	
Nerolidol (saturated in 90% PG)	-	-	60.8 [3.81]	68.9 [5.27]	n.s.c.	Lipid disruption/fluidisation	
Untreated	-	-	75	85	105	-	Leopold and Lippold (1995)
Oleic acid	-	-	40 (broadened)		-	Lipid fluidisation, partial lipid dissolution	
Oleic acid (10%) in dimethicone	-	-	35 (broadened)		-	-	
Highly purified light mineral oil	-	-	65	80	-	Lipid fluidisation, partial lipid dissolution	
Isopropyl myristate	-	-	60	80	-	Lipid fluidisation, partial lipid dissolution	
Caprylic/capric acid triglycerides containing 5% phospholipids	-	-	75	85	-	Lipid dissolution/extraction by inversed micelles of phospholipids	
Dibutyl adipate	-	-	70	80	-	Lipid dissolution/extraction	
Dimethicone 100	-	-	n.s.c.	n.s.c .	n.s.c.	No effect	
Cetearyl iso-octanoate	-	-	n.s.c.	n.s.c .	n.s.c.	No effect	
Caprylic/capric acid triglycerides	-	-	n.s.c.	n.s.c .	n.s.c.	No effect	
Untreated	36	51	72 [4.6 – 6.4]	83 [3.9 – 4.8]	100 [4.7 – 4.8]	-	Cornwell et al. (1996)
Limonene	-	-	51 [6]	66 [3.9]	106 [3.1]	Lipid disruption	

Nerolidol	-	-	68 [9]	80 [9.7]	109 [not measured]		
1,8-Cineole	-	-	48 [2.6]	68 [3.7]	107 [1.6]		
PG	-	-	70 [4.8]	79 [4.7]	-	No effect	
Limonene/PG	-	-	47 [5.2]	62 [3.5]	-	Lipid extraction	
Nerolidol/PG	-	-	65 [18]	77 [10]	-		
1-8-Cineole/PG	-	-	48 [1.3]	59 [3.4]	-		
Untreated	-	-	65	78	97	-	Vaddi et al. (2002a)
Ethanol (50%)	-	-	57	72	-	Lipid extraction, dehydration of SC protein	
Carvacrol (5%w/v in ethanol)	-	-	49	66	117	Lipid disruption/extraction, increased drug solubility in SC lipids	
Linalool (5%w/v in ethanol)	-	-	33	63	92	Lipid disruption/extraction, lipid fluidisation	
Terpineol (5%w/v in ethanol)	-	-	33	55	85		
Untreated	-	-	62	79	95	-	Vaddi et al. (2002b)
PG	-	-	58	76	-	Dehydration of SC protein	
Carvacrol (5%w/v in PG)	-	-	57	72	-	Lipid extraction, dehydration of SC protein	
Linalool (5%w/v in PG)	-	-	57	75.5	-	Lipid extraction, dehydration of SC protein	
Terpineol (5%w/v in PG)	-	-	57	75.5	105	Lipid extraction	
Untreated	-	-	62	79	95	-	Vaddi et al. (2003)
Ethanol (50%)	-	-	57	76	-	Lipid disruption/extraction, lipid fluidisation	
Limonene oxide (5%w/v in ethanol)	-	-	Broad endotherm		-	Lipid disruption/extraction	
Pinene oxide (5%w/v in ethanol)	-	-	31	52	-	Lipid disruption/extraction	

PG	-	-	58	76	-	Lipid disruption/extraction	
Limonene oxide (5%w/v in PG)	-	-	60	76	-	Lipid disruption/extraction	
Pinene oxide (5%w/v in PG)	-	-	56.5	73	-	Lipid disruption/extraction, lipid fluidisation	
Untreated	-	-	72.4	79.4	-	-	Winkler and Müller-Goymann (2005)
Water	-	-	70.0	77.4	-	-	
5-Aminolevulinic acid-n-butyl ester (5%w/v)	-	-	69.5	79.3	-	-	
5-Aminolevulinic acid (5%w/v)	-	-	70.0	77.2	-	-	
n-Butanol (1%v/v)	-	-	72.6	77.3	-	-	
Untreated	-	-	71.1	81.3	-	-	
Water	-	-	67.8	78.4	-	-	
Excipial® Fettcreme	-	-	67.5	75.6	-	-	
Excipial® Creme	-	-	66.8	77.3	-	-	
Basiscreme DAC (containing glyceryl monostearate 60, PEG-20-glyceryl stearate, cetylic alcohol, white petrolatum, propylene glycol, medium chain triglycerides and purified water)	-	-	66.5	76.7	-	-	
Dolgit® Mikrogel (containing 5% ibuprofen)	-	-	60.1	73.0	-	Lipid fluidisation	
Formulation containing Lutrol® F127 (poloxamer 407), dimethylisosorbide, isopropylic alcohol and purified water	-	-	63.9	77.2	-	-	
Formulation containing Lutrol® F127, dimethylisosorbide, ibuprofen acid, isopropylic alcohol and purified water	-	-	61.1	73.3	-	Lipid fluidisation	
Formulation containing Lutrol® F127, dimethylisosorbide, ibuprofen acid, isopropylic alcohol, medium chain triglycerides and purified water	-	-	60.1	73.1	-	Lipid fluidisation	
Untreated	-	-	68.61	80.28	-	-	Mitriaikina and Muller-Goymann (2007)
Wool fat alcohol ointment with betamethasone-17-valerate (0.1%w/v)	-	-	62.26	76.02	-	-	

Wool fat alcohol ointment with betamethasone-17-valerate (0.1%w/v) and isopropyl alcohol (5%w/v)	-	-	56.40, 64.14	74.18	-	Lipid extraction	
Isopropyl alcohol	-	-	64.14	-	-		
Isopropyl myristate	-	-	60.2	72.72	-	Modification of colloidal-crystal state of lipids, densification of SC	
Wool fat alcohol ointment with betamethasone-17-valerate (0.1%w/v), isopropyl alcohol (5%w/v) and isopropyl myristate (5%w/v)	-	-	61.3	70.6 – 72	-		
Untreated	-	-	65.23	75.59	-	-	
Basic cream DAC with betamethasone-17-valerate (0.1%w/v)	-	-	-	71.31	-	Hydration of keratin	
Basic cream DAC with betamethasone-17-valerate (0.1%w/v), isopropyl alcohol (5%w/v) and isopropyl myristate (5%w/v)	-	-	59.50	70.22	-	Modification of lipid structure	
Untreated	-	-	75	90	-	-	Kim et al. (2007)
n-Lauroyl sarcosine (2%w/v in 50%v/v ethanol)	-	-	66	79.5	-	Lipid fluidisation, lipid disordering	
Magainin (1 mM) and n-lauroyl sarcosine (2%w/v) in 50%v/v ethanol	-	-	65	78.5	-	Lipid fluidisation, lipid disordering	
Untreated	-	-	75	90	-	-	Kim et al. (2008)
n-Lauroyl sarcosine (1%w/v in PBS)	-	-	82	70	-	Lipid fluidisation, lipid disordering	
n-Lauroyl sarcosine (2%w/v in PBS)	-	-	66	79	-	Lipid fluidisation, lipid disordering	
n-Lauroyl sarcosine (3%w/v in PBS)	-	-	66	79	-	Lipid fluidisation, lipid disordering	
n-Lauroyl sarcosine (2%w/v in 25%v/v ethanol)	-	-	68	78	-	Lipid fluidisation	
n-Lauroyl sarcosine (2%w/v in 50%v/v ethanol)	-	-	66	79	-	Lipid fluidisation	
n-Lauroyl sarcosine (2%w/v in 75%v/v ethanol)	-	-	69	83	-	Lipid fluidisation	
n-Lauroyl sarcosine (2%w/v in 100%v/v ethanol)	-	-	70	85	-	Lipid fluidisation	
50%v/v ethanol	-	-	75	90	-	No effect	

Untreated (equilibrated with PBS)	-	-	53.2	78.1 – 84.1	-	-	Ibrahim and Li (2010)
n-Octanol	-	-	58.6	60 – 72.7	-	Lipid fluidisation	
1-Octyl-2-pyrrolidinone	-	-	36.2 – 54.3	66.6 – 71.5	-	Lipid fluidisation	
n-Dodecylpyrrolidinone	-	-	52.5 – 55.2		-	Lipid fluidisation	
2-Ethyl hexylsalicylate	-	-	55.4	77.9 – 86.7	-	-	
Isopropyl myristate	-	-	-	69.8 – 93.6	-	-	
Padimate O (2-Ethylhexyl 4-(dimethylamino)benzoate)	-	-	56.8	78.9 – 92.4	-	-	
Oleic acid	-	-	55.3	64.1-72.9	-	Lipid fluidisation	
Laurocapram (Azone™)	-	-	39	69.9 – 77.2	-	-	
Untreated	-	-	63	82	99.5	-	Kaushik and Michniak-Kohn (2010)
Ethanol	-	-	49	76	98	Lipid disruption/extraction	
PEG 400	-	-	70	84	-	Strengthening of SC lipids organisation and SC lipid–protein complex	
PG	-	-	61	76	-	Lipid disruption/extraction	
Laurocapram (Azone™)	-	-	-	69	-	Lipid disruption/extraction, protein extraction	
Laurocapram (0.4 M in water)	-	-	-	-	90, 98		
Laurocapram (0.4 M in ethanol)	-	-	58	84	90, 98		
Laurocapram (0.4 M in PEG 400)	-	-	58	82	-		
Laurocapram (0.4 M in PG)	-	-	57	-	92		
DMBIS (0.4 M in ethanol)	-	-	63	82	-		
DMBIS (0.4 M in PEG 400)	-	-	66	84	122		
DMBIS (0.4 M in PG)	-	-	56	72	86		

Untreated	-	-	70.87	83.51	-	-	Täuber and Müller-Goymann (2015)
Water	-	-	69.44	79.94	-	Lipid fluidisation	
PG	-	-	66.38	76.99	-	Increased lipid mobility (less compact microstructure)	
Medium chain triglyceride	-	-	54.45	70.83	-		
Isopropyl alcohol	-	-	71.30	83.35	-		
Selergo® 1% cream (1% ciclopirox)	-	-	63.69	74.47	-	-	
Formulation containing 10% poloxamer P407/medium chain triglyceride (4:1), 60% isopropyl alcohol/PG (2:1) and 30% water	-	-	53.24	67.02	-	-	

DMBIS: S,S-dimethyl-N-(4-bromobenzoyl) iminosulfurane; DMSO: dimethyl sulphoxide; n.s.c.: no significant changes; PEG: polyethylene glycol; PG: propylene glycol

Table 5 Modification of porcine SC transition temperatures following treatment with selected excipients and formulations used in topical and transdermal formulations

Excipient/Formulation	Average transition temperature (ºC), enthalpy (J/g) in square brackets where reported			Proposed actions	Reference
	T_2	T_3	T_4		
Untreated	62	75	105	-	Golden et al. (1987b)
Octadecanoic acid (0.15 M in ethanol)	62.5	Not reported	Not reported	No effect	
cis-6-Octadecenoic acid (0.15 M in ethanol)	60.5	Not reported	Not reported	Lipid disruption, reduced lipid orders	
cis-9-Octadecenoic acid (0.15 M in ethanol)	59	Not reported	Not reported		
cis-11-Octadecenoic acid (0.15 M in ethanol)	57	Not reported	Not reported		
trans-6-Octadecenoic acid (0.15 M in ethanol)	62	Not reported	Not reported	No/little effect	
trans-9-Octadecenoic acid (0.15 M in ethanol)	61.5	Not reported	Not reported		
trans-11-Octadecenoic acid (0.15 M in ethanol)	61	Not reported	Not reported		
Ethanol	62	Not reported	Not reported	No effect	
Untreated	60.4 [1.67]	72.5 [1.34]	100	-	Francoeur et al. (1990)
Ethanol (40%)	63.2 [1.05 J/g]	73.6 [1.09]	Not reported	Not reported	
Oleic acid (0.25% in 40% ethanol)	53.6 [1.13]	69.8 [0.75]	100	Lipid disruption	
Untreated (water)	-	63.0	81.0	-	Zhang and Lunter (2018)
Polysorbate 60 (5%)	-	63.7	81.5	-	
Cetyl stearyl alcohol (10%)	-	61.5	79.4	-	
Polysorbate 60 (5%) and cetyl stearyl alcohol (10%)	-	62.8	81.2	-	
Hydroxypropyl methyl cellulose (2.5%)	-	53.7	73.8	Disordered lipid conformation, perturbation of lipid lamellae packing	
Glycerol monostearate (4%)	-	54.6	76.8		
Polyoxyethylene-20-glycerol monostearate (7%)	-	53.8	72.1		

Cetearyl alcohol (and) sodium cetearyl sulfate (9%)	-	52.3	66.8		
Polyoxyethylene-20-glycerol monostearate (7%) and glycerol monostearate (4%)	-	55.7	70.0		
Sodium lauryl sulfate (1%)	-	50.7	62.5		
Non-ionic cream (polysorbate 60 (5%) and cetyl stearyl alcohol (10%))	-	58.5	76.3	-	
Anionic cream (cetearyl alcohol (and) sodium cetearyl sulfate (9%))	-	52.6	75.2	Effects on certain composition and complex structural arrangement of lipids	
Basic cream (polyoxyethylene-20-glycerol monostearate (7%) and glycerol monostearate (4%))		51.8	72.6		
Hydroxypropyl methyl cellulose and medium chain triglyceride emulsion	-	52.3	67.5	Increased SC fluidity	

Apart from changes in transition temperatures, Bouwstra et al. (1989) also noted that the observed transition enthalpy drop corresponded to an increase in skin permeability. *In vitro* skin permeation studies are usually conducted to confirm the skin permeability enhancement for drugs. This same study reported a drop in both the enthalpy of transition and transition temperatures after treatment with Azone™ analogs of varying chain lengths. Leopold and Lippold (1995) also related the reduced peak area (enthalpy) to the dissolution or extraction of the SC lipids following investigations with several lipid vehicles including mineral oil, isopropyl myristate and caprylic/capric acid triglycerides. Specifically, the enthalpic changes were only considered significant if such a difference was shown in ≥75% of the samples (n = 8 – 11) and the particular transition showed > 3ºC difference. In addition, the enthalpy ratios relative to the untreated samples were compared by Yamane et al. (1995a) to elucidate the degree of disruption in the lipid bilayers from the treatment of HSC with different terpenes and oleic acid for different time periods. The entropy change of the lipids was also monitored to assess the lipid fluidisation or reduction in the lipid order (Yamane et al., 1995b). A decrease in the entropy change was noted in the same study after treatment of HSC with different proportions of PG and water, especially for the T_2 peak but the effect decreased with a lower PG content. Cornwell et

al. (1996) and Vaddi et al. (2002a) added the peak sharpness (broadening) or cooperativity (peak broadening with an increased peak width at half height) as a supplementary observation to the lipid-related transitions, especially for the intercellular bilayers of the SC. A decrease in cooperativity means a reduced size of the cooperative units within the lipid bilayers. This was observed for both T_2 and T_3 peaks in the work by Cornwell et al. (1996) after treatment of HSC with several terpenes including limonene, nerolidol and 1,8-cineole. Vaddi et al. (2002a) reported the same results for T_1 to T_3 peaks following the application of different terpenes (carvacrol, linalool and terpineol) in ethanol on HSC. FTIR spectroscopic analysis confirmed the observations with a reduced peak area and a blue shift for both lipid and protein molecular vibrations. Later work by the same group reported similar observations for similar terpenes in PG as well as terpene oxides (limonene oxide and pinene oxide in PG or ethanol) (Vaddi et al., 2002b; Vaddi et al., 2003). Interestingly, limonene oxide in PG was found to increase the cooperativity of lipid endotherms probably due to an increased lipid bilayer cohesion. Tanojo et al. (1997) also reported a drop in the enthalpy (15 – 100 difference; unit not specified) for most of the samples of hydrated and dehydrated HSC at T_2 and T_3 transitions when treated with PG and its combination with several fatty acids except for nonanoic acid and linoleic acid (only for dehydrated sample) showing an increased enthalpy.

Most studies that have used DSC to understand the actions of certain excipients on the skin were conducted more than a decade ago. The application of DSC specifically to probe if some of these materials are potential skin penetration enhancers has been superseded by more sophisticated approaches. Table 4 and Table 5 includes results for excipients such as caprylic/capric acid triglycerides (Leopold and Lippold, 1995) that did not have any effects on skin thermal transitions. An early report by Williams and Barry (1990) disclosed that two terpenes (limonene and cineole) resulted in the same shift in thermal transitions of HSC. Of note, most of the investigations reported have also applied excess amounts of these materials to the skin. This clearly does not reflect typical application of topical or transdermal formulations in real life. Characterisation techniques such as FTIR spectroscopy (Curdy et al., 2004; Harrison et al., 1996a; Harrison et al., 1996b; Hasanovic et al., 2011; Ibrahim and Li, 2010; Kaushik and Michniak-Kohn, 2010), X-ray diffraction analysis (Cornwell et al., 1996; Cornwell et al., 1994; Marjukka Suhonen

et al., 1999; Schuckler et al., 1993), confocal Raman spectroscopy (Krombholz et al., 2021; Liu and Lunter, 2021; Lunter and Daniels, 2014; Mao et al., 2012; Patel et al., 2021; Zhang and Lunter, 2018) and nano-thermal analysis (Goh et al., 2017) have delivered new insights into the possible actions of such materials on the skin components and drug transport.

In addition to the typical lipid peaks, subzero lipid peaks, especially at -9ºC were also monitored to understand the effects of several excipients including PG, oleic acid and several fatty acids on transition temperatures and associated enthalpies of HSC (Tanojo et al., 1994, 1997; Tanojo et al., 1999). Following PG treatment this subzero peak (-10ºC) was absent in dehydrated HSC samples. The authors argued that the loss of this peak reflected a higher affinity of PG for water and a stronger interaction of PG with protein.

Apart from investigations of excipient actions on the SC, DSC has also been used to evaluate the influence of delivery systems and other treatments on the skin. Previously, Sznitowska et al. (2003) monitored the transition modification of HSC treated with buffers (pH 1 – 12). While most samples showed similar results to the control, alkaline-treated HSC showed a lowered T_2 transition (~72 to ~74ºC) with a reproducible decreased enthalpy of the T_3 peak. This suggested some degree of disordering of the lipid packing under the influence of alkaline pH. However, the resolution of the DSC curves presented was generally poor and no enthalpy values were reported.

Winkler and Müller-Goymann (2005) tested HSC samples with different drug solutions and formulations containing 5-aminolevulinic acid, 5-aminolevulinic acid-n-butyl ester and ibuprofen acid for DSC analysis. Most DSC data showed no major changes (>3ºC) except for commercialised (Dolgit® Mikrogel) and poloxamer-based formulations containing 5% of ibuprofen that showed a drop in both T_2 an T_3 transitions. These results were also supported by WAXD studies that revealed the presence of a reflection at 0.46 nm, corresponding to hydrocarbon chains in the liquid state. The lipid fluidisation contributed to a higher drug permeation observed.

The same group later applied DSC analysis for HSC samples treated with wool fat alcohol ointment and basic cream DAC (German Drug Code) containing 0.1%w/v of

betamethasone-17-valerate and two penetration enhancers (isopropyl alcohol (5%w/v) and isopropyl myristate (5%w/v)) (Mitriaikina and Muller-Goymann, 2007). For ointment-treated samples, the incorporation of individual penetration enhancers greatly reduced the T_2 an T_3 transitions than the ointment alone. This suggested a mutual interaction of penetration enhancers with the ointment base. Isopropyl alcohol showed lipid extraction effect that enhances the drug permeation. While, isopropyl myristate caused densification of the SC due to the modification of the colloidal-crystal state of lipids and this lowered the drug permeation. Synergistic effects were reported with enhanced drug permeation when both penetration enhancers were incorporated. DSC data showed a displacement of both transitions to lower temperatures and this could be due to the disorganisation of basic components of lipids in defined order and lipid fluidisation combined with protein denaturation. For cream-treated samples, the presence of water in the cream base causes significant changes to the thermal transitions (T_2 was not clearly detected; a minor shift for T_3). This was related to the hydration effect of keratin by the cream that causes the hydration of lipid polar head groups and swelling of the lipid layers. The addition of both penetration enhancers improved the drug permeation due to the synergistic effect aforementioned.

Later, Täuber and Müller-Goymann (2015) compared the transition change (T_2 an T_3) for HSC samples treated with different poloxamer 407 formulations containing ciclopirox and different excipients including isopropyl alcohol, PG and medium chain triglyceride. The study with only excipients alone showed medium chain triglyceride causes the highest shift of both transitions to lower temperatures. While, increasing isopropyl alcohol/PG and ciclopirox concentrations in the formulations showed higher transition shifts. This justified both excipients and drugs impacted the SC and reduce its permeation barrier function.

Zhang and Lunter (2018) attempted to study the influence of different emulsifiers (polysorbate 60, cetyl stearyl alcohol, glycerol monostearate, polyoxyethylene-20-glycerol monostearate, cetearyl alcohol (and) sodium cetearyl sulfate (CA-SCS) and sodium lauryl sulfate) and related emulsified formulations on the transition change of PSC. All of the emulsifiers (including mixed emulsifiers) showed a drop in both T_2 an T_3 transitions, especially anionic emulsifiers such as CA-SCS and sodium lauryl sulfate.

While, non-ionic emulsifiers such as polysorbate 60, cetyl stearyl alcohol and their combination demonstrated similar results as the untreated hydrated PSC. When the emulsifiers were formulated as creams and emulsions, similar observations were obtained as emulsifiers alone. In particular, hydroxypropyl methyl cellulose and medium chain triglyceride emulsion achieved the highest drop in the transitions. The presence of medium chain triglyceride increased lipid mobility and resulted a less compact microstructure.

Recently, Niu et al. (2019) applied DSC to observe the effect of Ethosomes (prepared with LIPOID S PC phosphatidylcholine and ethanol) on the delivery of donepezil hydrochloride (20mg/mL) in PSC. A drop in both transition temperature (T_2) at 60 – 70ºC and related enthalpy of PSC treated with the drug-loaded Ethosomes was observed. This was similar to an experiment repeated with an ethanolic solution (30%) containing the same drug content. The authors proposed that lipid disruption and fluidisation as reflected in the thermal events are possible mechanisms for Ethosomes to enhance drug permeation through the skin, primarily because of the presence of a high ethanol content. This is consistent with an earlier report by Kim et al. (2007) that examined the role of magainin (pore-forming peptide) and n-lauroyl sarcosine (anionic surfactant) on the thermal behaviour of HSC. A reduced transition temperature for T_2 and T_3 was observed for the investigated samples containing both excipients and a high percentage of ethanol (50%v/v). However, there was no comparison of samples with the individual excipients of interest and the role of each excipient was not further clarified. A further report by the same group later repeated the experiments by varying n-lauroyl sarcosine contents (1 – 3%w/v) in both PBS and ethanol (25 – 100%v/v). Transition temperature drops were reported for both excipients as observed in the previous study. It should be noted that it is unusual that HSC samples treated with 50%v/v ethanol showed no significant changes in both the T_2 and T_3 transitions.

5. Considerations for thermal characterisation of SC samples

Since the first use of thermal characterisation for SC samples, DSC has been extensively applied in monitoring the modification of thermal transitions (and endothermic enthalpies), especially in the 1990s. As we have noted in this review, the recent use of DSC in skin research is actually getting less attention. This may not be surprising because problems with data reproducibility have been consistently mentioned in several reports. However, we believe this issue to be related to the sensitivity and resolution of DSC analysis. The question arising now is whether there is a standard experimental protocol for robust and reliable thermal analysis of the SC?

Unlike the typical use of DSC for thermal characterisation of pharmaceutical ingredients including drugs, the composition of organic tissues such as the SC is complicated. In addition, the different sources of skin samples including but not limited to donor gender, age, body locations and species (for porcine skin) can contribute substantially to the wide range of transitions reported in the literature. These are additional challenges as well as the various experimental and instrumental variables. We suggest that the comparisons within the same experiment (especially with different treatments) shall be made using the same donor and body part to reduce the results variations.

Nonetheless, our experience with unpublished data shared via this review has identified two very critical parameters that require consideration – heating rate and pan type. A heating rate of 10ºC/min or lower is generally used but we recommend 2ºC/min as a starting point to obtain DSC profiles with optimal resolution and sensitivity. We attempted MTDSC that may improve the detection of the low enthalpic transition such as the T_1 peak, but conventional DSC is adequate for routine experiments. In addition, a closed pan system such as the hermetically sealed pan is recommended in studying the interactions of skin lipids and proteins, especially those transitions with a low enthalpy. Good contact between sample and pan must be established for acceptable DSC analysis and a sufficient sample size is, thus, needed. Of course, the sample mass will depend on the pan size (volume) and a load of 3 – 5 mg of SC for a 40 µL pan appears appropriate. Folding the SC sheets can help in loading a decent amount of sample into the pan. Care must be taken to attempt loading the samples (especially hydrated) into the pan within a

short period (up to 15 min) to prevent the loss of moisture. Considering the irregular baselines that may impede proper analysis, we also suggest that operators increase the number of samples measured where necessary.

The treatment period with excipients or formulations varying from 30 min to 48 h has been reported. The time shall be determined based on the purpose of studies but several reports have showed the same effect can be studied by just incubating SC samples with only 30 min at room temperature (Mitriaikina and Muller-Goymann, 2007; Winkler and Müller-Goymann, 2005). Hydration of the SC with 20 – 40% of water content is recommended especially for HSC prior to the treatment to mimic the *in vivo* hydration level of the SC (Potts, 1986) and allow better detection of the related transitions.

DSC analysis through monitoring peak enthalpy and cooperativity can assist in comparing the action and extent of a particular treatment or application of an excipient or formulation to the skin. It must be emphasised that most studies have compared data qualitatively by monitoring the changes in the DSC curves. There are only several reports quantifying the actual enthalpy values of the endothermic peaks but a huge variation is noticed. It remains extremely challenging to evaluate properly the enthalpy given that the baseline is irregular and differs among samples. It is also important to note that most of the published studies are worth revisiting considering the large amounts of excipients to which skin samples are exposed. Exposure or incubation with amounts of formulations or excipients typically applied *in vivo* in humans is strongly recommended for accurate interpretation of data. With this approach, we believe that the potential of DSC as a robust analytical tool in skin research will be further expanded.

6. Conclusion

Over five decades, the use of thermal analysis, specifically DSC has opened up new vistas in skin research that have contributed important insights regarding our understanding of skin barrier function. Even though DSC has been a popular tool for skin research over the years, greater attention must be given to study design, especially experimental and instrumental variables, as highlighted in the current review. Routine

monitoring of thermotropic transitions has also been a simple and rapid identification method for possible modification of skin components, especially skin lipids and protein. We believe that experimental and instrumental variables must be carefully selected before appropriate comparisons with DSC analysis from different treatments can be realised. With this, we recommend the following experimental and instrumental variables as a good starting point for DSC analysis with SC samples:

- Pan type: Hermetically sealed pan
- Sample mass: 3 – 5 mg (40 µL pan)
- Heating rate: 10ºC/min or lower (2ºC/min for higher resolution and sensitivity)
- Temperature range: 0 – 140°C
- Number of samples: at least 3 to 5

Acknowledgement

The authors would like to thank Prof. Dr Duncan Q.M. Craig for his supervision and valuable comments for the current review.

Declaration of competing interest

The authors declare that they have no known competing financial interests or personal relationships that could have appeared to influence the work reported in this paper.

References

Al-Saidan, S.M., Barry, B.W., Williams, A.C., 1998. Differential scanning calorimetry of human and animal stratum corneum membranes. Int J Pharm 168, 17-22.

Barry, B.W., 1987. Mode of action of penetration enhancers in human skin. J. Control. Release 6, 85-97.

Bouwstra, J.A., de Vries, M.A., Gooris, G.S., Bras, W., Brussee, J., Ponec, M., 1991a. Thermodynamic and structural aspects of the skin barrier. J. Control. Release 15, 209-219.

Bouwstra, J.A., Gooris, G.S., 2010. The Lipid Organisation in Human Stratum Corneum and Model Systems. Open Dermatol. J. 4, 10-13.

Bouwstra, J.A., Gooris, G.S., Bras, W., Downing, D.T., 1995. Lipid organisation in pig stratum corneum. J. Lipid Res. 36, 685-695.

Bouwstra, J.A., Gooris, G.S., van der Spek, J.A., Bras, W., 1991b. Structural investigations of human stratum corneum by small-angle X-ray scattering. J. Investig. Dermatol. 97, 1005-1012.

Bouwstra, J.A., Gooris, G.S., Vries, M.A.S., van der Spek, J.A., Bras, W., 1992. Structure of human stratum corneum as a function of temperature and hydration: A wide-angle X-ray diffraction study. Int J Pharm 84, 205-216.

Bouwstra, J.A., Peschier, L.J.C., Brussee, J., Boddé, H.E., 1989. Effect of n-alkyl-azocycloheptan-2-ones including azone on the thermal behaviour of human stratum corneum. Int J Pharm 52, 47-54.

Bulgin, J.J., Vinson, L.J., 1967. The use of differential thermal analysis to study the bound water in stratum corneum membranes. Biochim Biophys Acta Gen 136, 551-560.

Caussin, J., Gooris, G.S., Janssens, M., Bouwstra, J.A., 2008. Lipid organization in human and porcine stratum corneum differs widely, while lipid mixtures with porcine ceramides model human stratum corneum lipid organization very closely. Biochim Biophys Acta Biomembr 1778, 1472-1482.

Chapman, D., 1975. Phase transitions and fluidity characteristics of lipids and cell membranes. Q. Rev. Biophys. 8, 185-235.

Coleman, N.J., Craig, D.Q.M., 1996. Modulated temperature differential scanning calorimetry: A novel approach to pharmaceutical thermal analysis. Int J Pharm 135, 13-29.

Cornwell, P.A., Barry, B.W., Bouwstra, J.A., Gooris, G.S., 1996. Modes of action of terpene penetration enhancers in human skin: Differential scanning calorimetry, small-angle X-ray diffraction and enhancer uptake studies. Int J Pharm 127, 9-26.

Cornwell, P.A., Barry, B.W., Stoddart, C.P., Bouwstra, J.A., 1994. Wide-angle X-ray diffraction of human stratum corneum: Effects of hydration and terpene enhancer treatment. J. Pharm. Pharmacol. 46, 938-950.

Curdy, C., Naik, A., Kalia, Y.N., Alberti, I., Guy, R.H., 2004. Non-invasive assessment of the effect of formulation excipients on stratum corneum barrier function *in vivo*. Int J Pharm 271, 251-256.

de Vos, A.M., Kinget, R., 1993. Study of the penetration-enhancing effect of two nonionic surfactants (Cetiol® HE and eumulgin® B3) on human stratum corneum using differential scanning calorimetry. Eur. J. Pharm. Sci. 1, 89-93.

Duzee, B.F.V., 1975. Thermal analysis of human stratum corneum. J. Investig. Dermatol. 65, 404-408.

Francoeur, M., Golden, G., Potts, R., 1990. Oleic acid: Its effects on stratum corneum in relation to (trans)dermal drug delivery. Pharm Res 7, 621-627.

Gay, C.L., Guy, R.H., Golden, G.M., Mak, V.H.W., Francoeur, M.L., 1994. Characterization of low-temperature (i.e., <65ºC) lipid transitions in human stratum corneum. J. Investig. Dermatol. 103, 233-239.

Goh, C.F., Moffat, J.G., Craig, D.Q.M., Hadgraft, J., Lane, M.E., 2017. Nano-thermal imaging of the stratum corneum and its potential use for understanding of the mechanism of skin penetration enhancer. Thermochim Acta 655, 278-283.

Golden, G.M., Guzek, D.B., Harris, R.R., McKie, J.E., Potts, R.O., 1986. Lipid thermotropic transitions in human stratum corneum. J. Investig. Dermatol. 86, 255-259.

Golden, G.M., Guzek, D.B., Kennedy, A.E., McKie, J.E., Potts, R.O., 1987a. Stratum corneum lipid phase transitions and water barrier properties. Biochemistry 26, 2382-2388.

Golden, G.M., McKie, J.E., Potts, R.O., 1987b. Role of stratum corneum lipid fluidity in transdermal drug flux. J. Pharm. Sci. 76, 25-28.

Goodman, M., Barry, B.W., 1986. Differential scanning calorimetry of human stratum corneum: Effects of penetration enhancers azone and dimethyl sulphoxide. Anal. Proc. 23, 397-398.

Harrison, J., Watkinson, A., Green, D., Hadgraft, J., Brain, K., 1996a. The Relative Effect of Azone® and Transcutol® on Permeant Diffusivity and Solubility in Human Stratum Corneum. Pharm Res 13, 542-546.

Harrison, J.E., Groundwater, P.W., Brain, K.R., Hadgraft, J., 1996b. Azone® induced fluidity in human stratum corneum. A Fourier transform infrared spectroscopy investigation using the perdeuterated analogue. J. Control. Release 41, 283-290.

Hasanovic, A., Winkler, R., Resch, G.P., Valenta, C., 2011. Modification of the conformational skin structure by treatment with liposomal formulations and its correlation to the penetration depth of aciclovir. Eur. J. Pharm. Biopharm. 79, 76-81.

Ibrahim, S.A., Li, S.K., 2010. Chemical enhancer solubility in human stratum corneum lipids and enhancer mechanism of action on stratum corneum lipid domain. Int J Pharm 383, 89-98.

Kaushik, D., Michniak-Kohn, B., 2010. Percutaneous penetration modifiers and formulation effects: Thermal and spectral analyses. AAPS PharmSciTech 11, 1068-1083.

Khan, Z.U., Kellaway, I.W., 1989. Differential scanning calorimetry of dimethylsulphoxide-treated human stratum corneum. Int J Pharm 55, 129-134.

Kim, Y.-C., Ludovice, P.J., Prausnitz, M.R., 2007. Transdermal delivery enhanced by magainin pore-forming peptide. J. Control. Release 122, 375-383.

Kim, Y.-C., Park, J.-H., Ludovice, P.J., Prausnitz, M.R., 2008. Synergistic enhancement of skin permeability by N-lauroylsarcosine and ethanol. Int J Pharm 352, 129-138.

Knutson, K., Potts, R.O., Guzek, D.B., Golden, G.M., McKie, J.E., Lambert, W.J., Higuchi, W.I., 1985. Macro- and molecular physical-chemical considerations in understanding drug transport in the stratum corneum. J. Control. Release 2, 67-87.

Krombholz, R., Liu, Y., Lunter, D.J., 2021. In-Line and Off-Line Monitoring of Skin Penetration Profiles Using Confocal Raman Spectroscopy. Pharmaceutics 13, 67.

Ladbrooke, B.D., Chapman, D., 1969. Thermal analysis of lipids, proteins and biological membranes. A review and summary of some recent studies. Chem. Phys. Lipids 3, 304-356.

Leopold, C.S., Lippold, B.C., 1995. An attempt to clarify the mechanism of the penetration enhancing effects of lipophilic vehicles with differential scanning calorimetry (DSC). J. Pharm. Pharmacol. 47, 276-281.

Lever, T., 2007. Optmizing DSC experiments, in: Craig, D.Q.M., Reading, M. (Eds.), Thermal Analysis of Pharmaceuticals. CRC Press, Boca Raton, pp. 23-52.

Lin, S.Y., Duan, K.J., Lin, T.C., 1996. Simultaneous determination of the protein conversion process in porcine stratum corneum after pretreatment with skin enhancers by a combined microscopic FT-IR/DSC system. Spectrochim. Acta A 52, 1671-1678.

Lin, S.Y., Liang, R.C., Lin, T.C., 1994. Lipid and protein thermotropic transition of porcine stratum corneum by microscopic calorimetry and infrared spectroscopy. J Chin Chem Soc 41, 425-429.

Liu, Y., Lunter, D.J., 2021. Profiling skin penetration using PEGylated emulsifiers as penetration enhancers via confocal Raman spectroscopy and fluorescence spectroscopy. Eur. J. Pharm. Biopharm. 166, 1-9.

Lunter, D., Daniels, R., 2014. Confocal Raman microscopic investigation of the effectiveness of penetration enhancers for procaine delivery to the skin. J. Biomed. Opt. 19, 126015.

Mak, V.W., Potts, R., Guy, R., 1991. Does hydration affect intercellular lipid organization in the stratum corneum? Pharm Res 8, 1064-1065.

Mao, G., Flach, C.R., Mendelsohn, R., Walters, R.M., 2012. Imaging the Distribution of Sodium Dodecyl Sulfate in Skin by Confocal Raman and Infrared Microspectroscopy. Pharm Res 29, 2189-2201.

Marjukka Suhonen, T., A. Bouwstra, J., Urtti, A., 1999. Chemical enhancement of percutaneous absorption in relation to stratum corneum structural alterations. J. Control. Release 59, 149-161.

Mitriaikina, S., Muller-Goymann, C.C., 2007. Synergetic effects of isopropyl alcohol (IPA) and isopropyl myristate (IPM) on the permeation of betamethasone-17-valerate from semisolid Pharmacopoeia bases. Journal of Drug Delivery Science and Technology 17, 1-8.

Niu, X.-Q., Zhang, D.-P., Bian, Q., Feng, X.-F., Li, H., Rao, Y.-F., Shen, Y.-M., Geng, F.-N., Yuan, A.-R., Ying, X.-Y., Gao, J.-Q., 2019. Mechanism investigation of ethosomes transdermal permeation. In J Pharm 1, 100027.

Park, J.H., Lee, J.W., Kim, Y.C., Prausnitz, M.R., 2008. The effect of heat on skin permeability. Int J Pharm 359, 94-103.

Patel, A., Iliopoulos, F., Caspers, P.J., Puppels, G.J., Lane, M.E., 2021. In Vitro–In Vivo Correlation in Dermal Delivery: The Role of Excipients. Pharmaceutics 13, 542.

Ponec, M., Weerheim, A., Lankhorst, P., Wertz, P., 2003. New Acylceramide in Native and Reconstructed Epidermis. J. Investig. Dermatol. 120, 581-588.

Potts, R.O., 1986. Stratum corneum hydration: experimental techniques and interpretations of results. Journal of The Society of Cosmetic Chemists 37, 9-33.

Pouliot, R., Germain, L., Auger, F.A., Tremblay, N., Juhasz, J., 1999. Physical characterization of the stratum corneum of an *in vitro* human skin equivalent produced by tissue engineering and its comparison with normal human skin by ATR-FTIR spectroscopy and thermal analysis (DSC). Biochim Biophys Acta Mol Cell Biol Lipids 1439, 341-352.

Rehfeld, S.J., Plachy, W.Z., Williams, M.L., Elias, P.M., 1988. Calorimetric and electron spin resonance examination of lipid phase transitions in human stratum corneum: Molecular basis for normal cohesion and abnormal desquamation in recessive X-linked ichthyosis. J. Investig. Dermatol. 91, 499-505.

Sandu, C., Singh, R.K., 1990. Modeling differential scanning calorimetry. Thermochim Acta 159, 267-298.

Schuckler, F., Bouwstra, J.A., Goons, G.S., Lee, G., 1993. An X-ray diffraction study of some model stratum corneum lipids containing Azone and dodecyl-L-pyroglutamate. J. Control. Release 23, 27-36.

Silva, C.L., Nunes, S.C.C., Eusébio, M.E.S., Pais, A.A.C.C., Sousa, J.J.S., 2006a. Thermal behaviour of human stratum corneum. Skin Pharmacol. Physiol. 19, 132-139.

Silva, C.L., Nunes, S.C.C., Eusébio, M.E.S., Sousa, J.J.S., Pais, A.A.C.C., 2006b. Study of human stratum corneum and extracted lipids by thermomicroscopy and DSC. Chem. Phys. Lipids 140, 36-47.

Sznitowska, M., Janicki, S., Williams, A., Lau, S., Stołyhwo, A., 2003. pH-induced modifications to stratum corneum lipids investigated using thermal, spectroscopic, and chromatographic techniques. J. Pharm. Sci. 92, 173-179.

Tanojo, H., Bouwstra, J.A., Junginger, H.E., Boddé, H.E., 1994. Subzero thermal analysis of human stratum corneum. Pharm Res 11, 1610-1616.

Tanojo, H., Bouwstra, J.A., Junginger, H.E., Boddé, H.E., 1997. *In vitro* human skin barrier modulation by fatty acids: Skin permeation and thermal analysis studies. Pharm Res 14, 42-49.

Tanojo, H., Bouwstra, J.A., Junginger, H.E., Boddé, H.E., 1999. Thermal analysis studies on human skin and skin barrier modulation by fatty acids and propylene glycol. J. Therm. Anal. Calorim. 57, 313-322.

Täuber, A., Müller-Goymann, C.C., 2015. In vitro model of infected stratum corneum for the efficacy evaluation of poloxamer 407-based formulations of ciclopirox olamine against Trichophyton rubrum as well as differential scanning calorimetry and stability studies. Int J Pharm 494, 304-311.

Vaddi, H.K., Ho, P.C., Chan, Y.W., Chan, S.Y., 2002a. Terpenes in ethanol: haloperidol permeation and partition through human skin and stratum corneum changes. J. Control. Release 81, 121-133.

Vaddi, H.K., Ho, P.C.L., Chan, S.Y., 2002b. Terpenes in propylene glycol as skin-penetration enhancers: Permeation and partition of haloperidol, Fourier transform infrared spectroscopy, and differential scanning calorimetry. J. Pharm. Sci. 91, 1639-1651.

Vaddi, H.K., Ho, P.C.L., Chan, Y.W., Chan, S.Y., 2003. Oxide terpenes as human skin penetration enhancers of haloperidol from ethanol and propylene glycol and their modes of action on stratum corneum. Biol. Pharm. Bull 26, 220-228.

Walkley, K., 1972. Bound water in stratum corneum measured by differential scanning calorimetry. J. Investig. Dermatol. 59, 225-227.

Wertz, P.W., Downing, D.T., 1983a. Acylglucosylceramides of pig epidermis: structure determination. J. Lipid Res. 24, 753-758.

Wertz, P.W., Downing, D.T., 1983b. Ceramides of pig epidermis: structure determination. J. Lipid Res. 24, 759-765.

Wilkes, G.L., Nguyen, A.-L., Wildnauer, R., 1973. Structure-property relations of human and neonatal rat stratum corneum I. Thermal stability of the crystalline lipid structure as studied by X-ray diffraction and differential thermal analysis. Biochim Biophys Acta Gen 304, 267-275.

Williams, A., Barry, B., 1990. Differential Scanning Calorimetry Does Not Predict the Activity of Terpene Penetration Enhancers in Human Skin. J. Pharm. Pharmacol. 42, 156P-156P.

Winkler, A., Müller-Goymann, C.C., 2005. The influence of topical formulations on the permeation of 5-aminolevulinic acid and its n-butyl ester through excised human stratum corneum. Eur. J. Pharm. Biopharm. 60, 427-437.

Yamane, M.A., Williams, A.C., Barry, B.W., 1995a. Effects of terpenes and oleic acid as skin penetration enhancers towards 5-fluorouracil as assessed with time: Permeation, partitioning and differential scanning calorimetry. Int J Pharm 116, 237-251.

Yamane, M.A., Williams, A.C., Barry, B.W., 1995b. Terpene penetration enhancers in propylene glycol/water co-solvent systems: Effectiveness and mechanism of action. J. Pharm. Pharmacol. 47, 978-989.

Zhang, Z., Lunter, D.J., 2018. Confocal Raman microspectroscopy as an alternative to differential scanning calorimetry to detect the impact of emulsifiers and formulations on stratum corneum lipid conformation. Eur. J. Pharm. Sci. 121, 1-8.